MINISTÉRIO DA CIÊNCIA E TECNOLOGIA
INSTITUTO NACIONAL DE PESQUISAS ESPACIAIS

Numerical Simulation and Data Analysis
Brazilian Lab for Computing and Applied Mathematics

Núcleo para Simulação e Análise de Sistemas Complexos (NUSASC/GPesq)
Laboratório Associado de Computação e Matemática Aplicada (LAC)
Centro de Tecnologias Especiais (CTE) – INPE – São José dos Campos-SP-Brazil
reinaldo@lac.inpe.br / reinaldo.rosa@pq.cnpq.br / www.lac.inpe.br

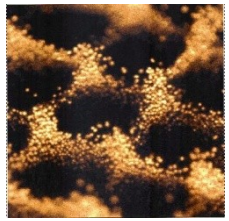

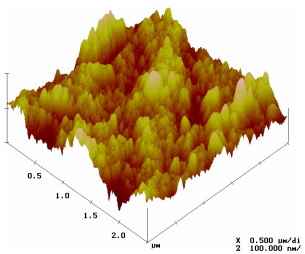

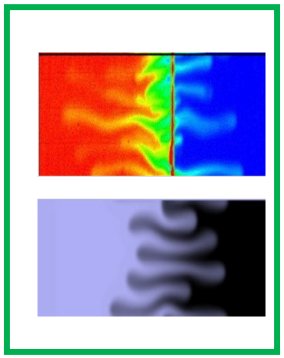

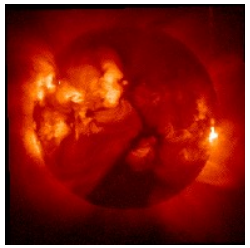

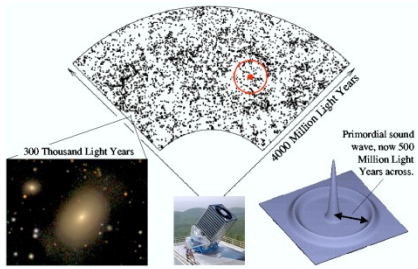

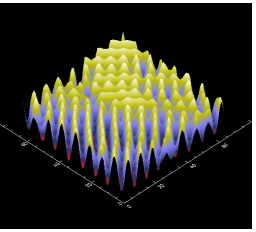

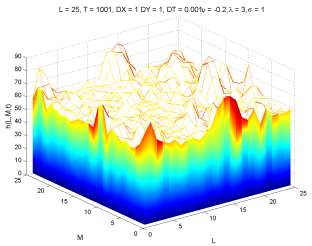

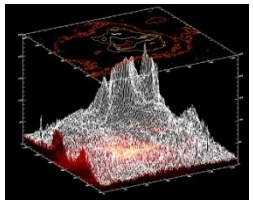

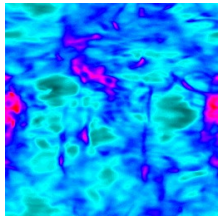

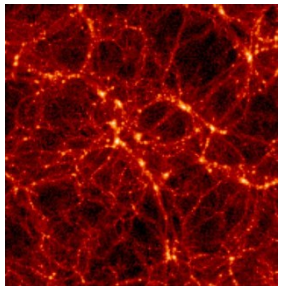

NUSASC_LAC_INPE

Elbert E.N. Macau
Fernando M. Ramos
Haroldo F.C. Velho
Hanumant Sawant
Luis Bambace
Margerete Domingues
Reinaldo R. Rosa

Ademilson Zanandrea
Ana Paula Andrade
Cesar Caretta
Maurício Bolzan

Mariana Baroni
Noemio Xavier
Gustavo Zaniboni
Ramon Freitas
Silas Bianchi
Thalita Veronese

Eduardo Charles
Juliana M. Guerra
Laurita dos Santos
Murilo Dantas

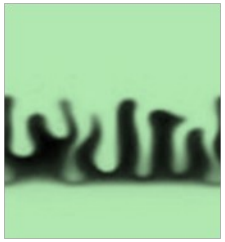

Anne De Wit (ULB)
Antonio F. da Silva (UFBA)
Arcilan Assireu (INPE/USP)
Christo Christov (Lousiana)
Harry Swinney (UTA)
José Pontes (UFRJ)
Marcus Hauser (Magdeburg)
Marian Karlick (Ondrejov)
Surjalal Sharma (Maryland)

EX. de Sistema Simples
Equação da Membrana
(Coordenadas Polares)

$$A_{tt} = (1/c^2)\,(A_{rr} + r^{-1} A_r + r^{-2} A_{\theta\theta})$$

A(t,r,θ) é um deslocamento ➔ uma solução (EDO) para a variável radial

Prova-se, analiticamente, que existe uma família de funções que admitem Soluções do tipo:

$$S_{n,k}(t,r,\theta) = J_n(b_{n,k})\,\cos(n\theta t)$$ (*Funções Especiais de Bessel*)

Onde n indica a quantidade de *diâmetros nodais* e k a ordem da função.

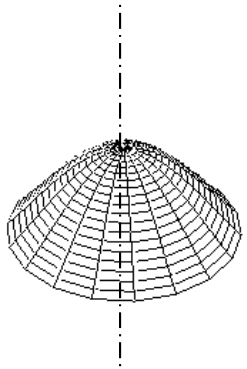

ELSEVIER

Physica A 283 (2000) 156–159

PHYSICA A

www.elsevier.com/locate/physa

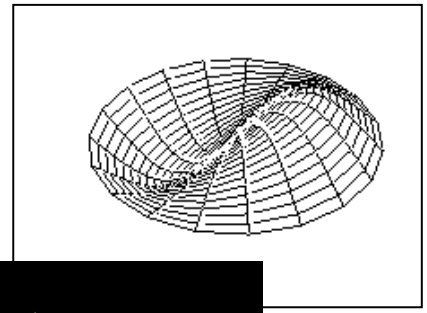

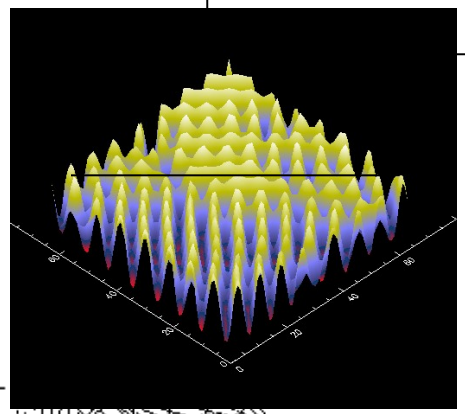

Gradient pattern analysis of Swift–Hohenberg dynamics: phase disorder characterization

R.R. Rosa[a,*], J. Pontes[b], C.I. Christov[d,1], F.M. Ramos[a], C. Rodrigues Neto[a], E.L. Rempel[a], D. Walgraef[c]

[a]*LAC-INPE, National Institute for Space Research-INPE, P.O.Box 515, 12201-970, São José dos Campos, SP Brazil*

[b]*COPPE, UFRJ, Rio de Janeiro, Brazil*

[c]*CNPCS, Université Libre de Bruxelles, Belgium*

[d]*Institut Pluridisciplinar, Universidad Complutense, Madrid, Spain*

Abstract

In this paper, we analyze the onset of phase-dominant dynamics in a uniformly forced system. The study is based on the numerical integration of the Swift–Hohenberg equation and adresses the characterization of phase disorder detected from gradient computational operators as complex entropic form (CEF). The transition from amplitude to phase dynamics is well characterized by means of the variance of the CEF phase component. © 2000 Elsevier Science B.V. All rights reserved.

PACS: 02.90.+p; 05.45.Pq; 05.45.Tp; 05.70.Ln; 47.20.Ky; 47.54.+r

Keywords: Extended systems; Pattern formation; Gradient dynamics; Complex Entropic form; Phase disorder

$$A_{tt} = (1/c^2)\,(A_{rr} + r^{-1}\,A_r + r^{-2}\,A_{\theta\theta})$$

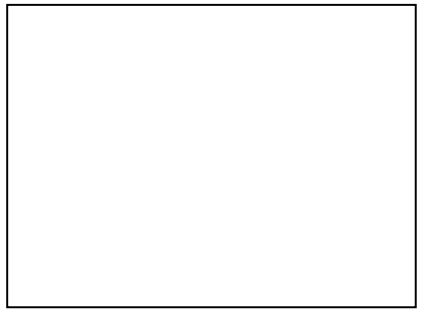

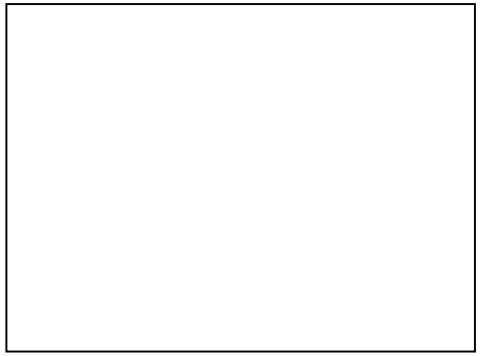

CCIS 2010

Numerical Simulation and Computational Analysis of Miscible Displacement Flows

R.R.Rosa (LAC-INPE), M.PA. Baroni (UFABC)
and A. de Wit (ULB)

Outline:

- Equations & Numerical Solutions
- Simulation, Analysis and Interpretation
- Advanced Applications (Short Chaotic Time Series)

EQUATIONS:

- Two miscible different solutions in contact at t=0
- The density (ρ) or viscosity (μ) depends on the solute concentration *c*

➔ *Darcy´s* description: velocity field + convection-diffusion equation for *c*

- The model is a two-dimensional porous medium or thin Hele-Shaw cell of length L_x and width L_y, containing a stratification of two miscible solutions of species *c*.
- The system can be described by Darcy's law for the velocity field $\underline{u} = (u, v)$ coupled to a convection-diffusion equation for the concentration of species c [a] :

$$\underline{\nabla} \cdot \underline{u} = 0 \qquad (1)$$

$$\underline{\nabla} p = -\frac{\mu}{\kappa}\underline{u} + \rho \underline{g} \qquad (2)$$

$$\frac{\partial c}{\partial t} + \underline{u} \cdot \underline{\nabla} c = D\nabla^2 c \qquad (3)$$

where the permeabiblity κ and diffusion coefficient D are constants, while p represents the pressure, μ represents the viscosity and ρ represents the density.

- For viscous fingering formation : the gravity term is neglected and the viscosity μ depends on *c*.
- For density fingering formation : the gravity field $\underline{g}$ is oriented along *x* and the density ρ depends of *c*. The solution with concentration $c = 0$ have density ρ_0, where $\rho_0 > \rho_1$, and the viscosity μ is constant.

a. G. M. Homsy, "*Ann. Rev. Fluid Mech.*" **19**, 271 (1987).

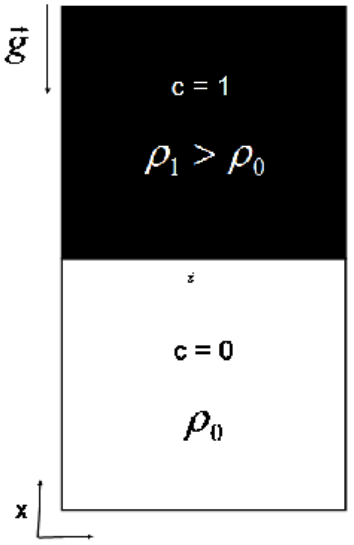

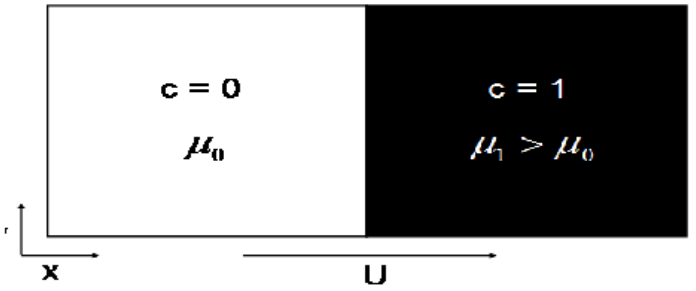

Dimensionless equations

- Using U as the characteristic velocity, it is possible non-dimensionalize the governing equations using $L = \frac{D}{U}$ as length scale and $\tau = \frac{D}{U^2}$ as time scale.
- Introducing the stream function $\psi(x, y)$ such as $u = \frac{\partial \psi}{\partial y}$ and $v = \frac{-\partial \psi}{\partial x}$ and after some algebra, we obtain the final dimensionless equations :

For density fingering :

$$\nabla^2 \psi = w, \quad (4)$$

$$w = R_a(c_y), \quad (5)$$

$$\frac{\partial c}{\partial t} + c_x \psi_y - c_y \psi_x = \nabla^2 c \quad (6)$$

For viscous fingering :

$$\nabla^2 \psi = w \quad (7)$$

$$w = R(c_x \psi_x + c_y \psi_y + c_y), \quad (8)$$

$$\frac{\partial c}{\partial t} + c_x \psi_y - c_y \psi_x = \nabla^2 c \quad (9)$$

- Analyzing the final dimensionless equations for both cases, we can see the difference is in the term $w(x, y)$.
- This term for viscous fingering shows that the vorticity is generated by mobility (concentration) gradients not perpendicular to the flow [1].

1. G. M. Homsy, "*Ann. Rev. Fluid Mech.*" **19**, 271 (1987).

NUMERICAL SIMULATIONS:

- R=Ra=3 (canonical unstable case)
- Pseudo-spectral method (Tan & Homsy, Phys. Fluids 29, 3549, 1986)
- Periodic BC in x and y
- IC: ψ=0 for all (x,y) and two back to back step functions between c=1 and c=0 with c=1/2 + A.r with $r \in (0,1)$, A=noise amplitude
- Systems length: Lx=4096 and Ly=1024
- Spatial discretization uses a dimensioless ratio of 4 between the number of spectral modes
- Time discretization: 0.2 (0-2000)

- The linear stability analysis for viscous fingering provide the dispersion curve where the growth rate σ of the perturbations as a function of their wavenumbe k [2] :

$$\sigma = \frac{1}{2}\left[(Rk - k^2) - \sqrt{k(k^2 + 2Rk)}\right].$$

For times $t > 0$, solving numerically by taking the limit of $t \longrightarrow 0$, the growth constant is maximum at $t = 0$ and decays with time.

- The linear stability analysis for density fingering is obtained in a similar way [3] :

$$\sigma = \frac{k}{2}\left(R_a - k - \sqrt{k[k + 2(R_a)]}\right)$$

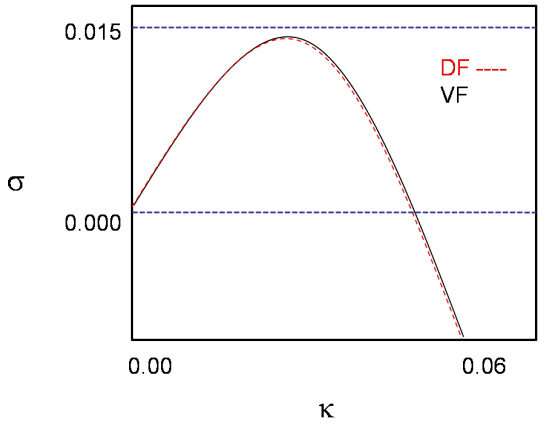

Structural Measures on Averaged Profiles

The transverse average profile is given by

$$\langle c(x,t)\rangle = \frac{1}{L_y}\int_0^{L_y} c(x,y,t)dy$$

and correponds to standard curves computed in fingerings studies

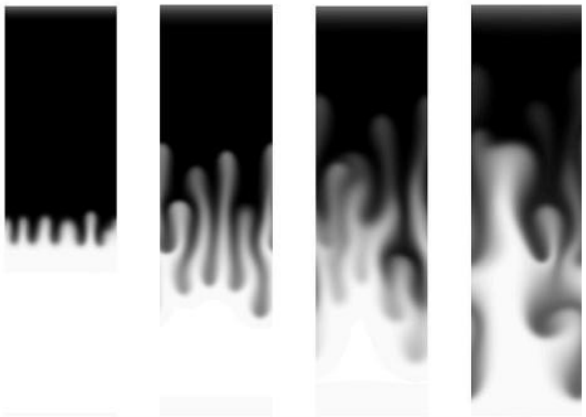

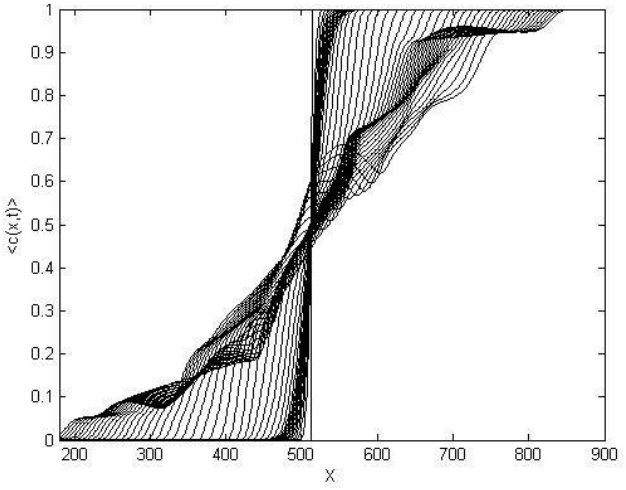

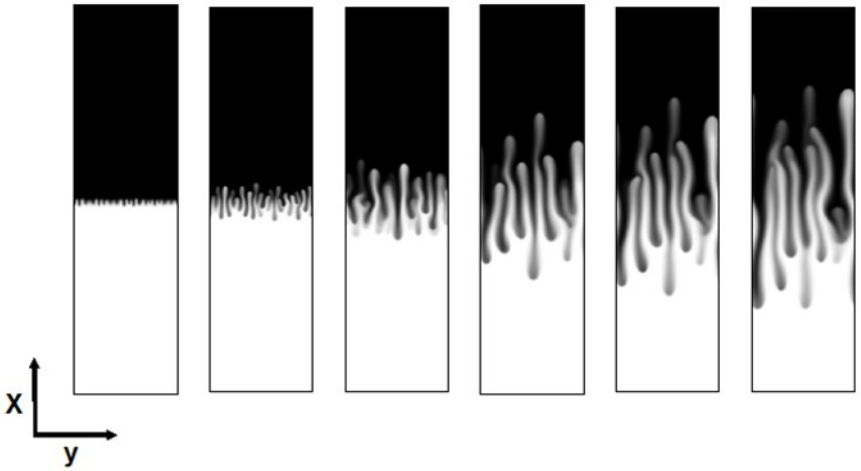

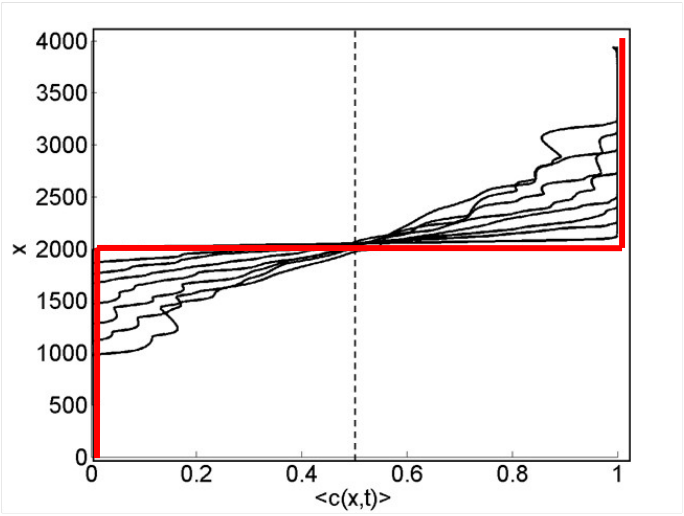

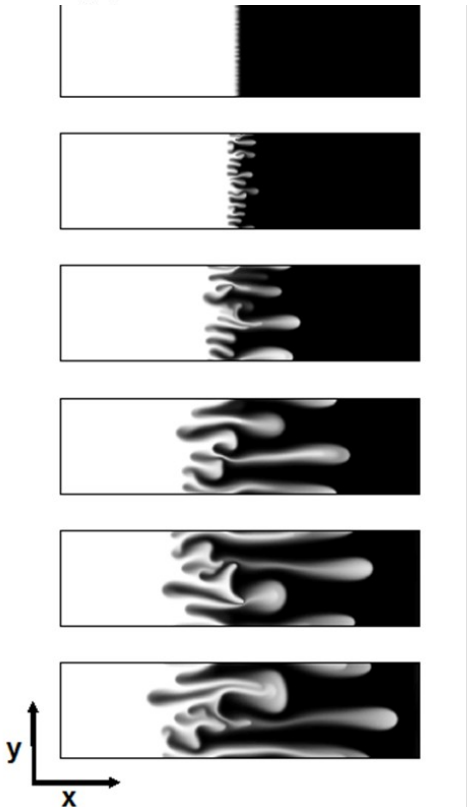

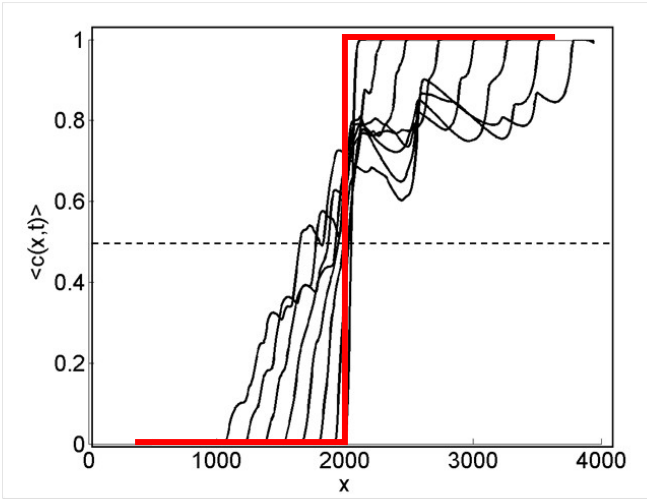

“Bilateral asymmetry”

DATA ANALYSIS

Structural Measurements

- Mixing Length : L=distance between the tip and rear of the fingers (spatio extent of the mixing zone)

- Statistical skewness: $$S(t) = \left(\frac{\sum_x (\langle c(x_i) \rangle - \overline{\langle c \rangle})^3}{\sum_x (\langle c(x_i) \rangle - \overline{\langle c \rangle})^{3/2}} \right)_t$$

(scaling richness)

- Gradient Asymmetry Coefficient: $G_A = (Nc - Nv)/Nv$

(coarsening and side-finger instability)

Gradient Pattern Analysis

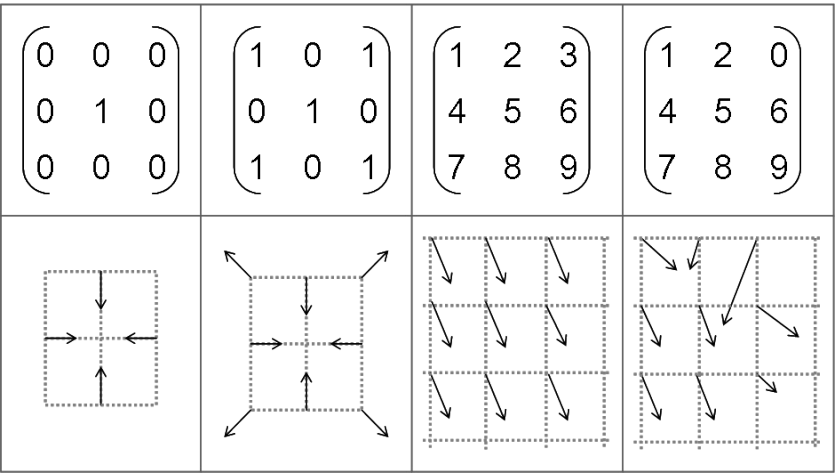

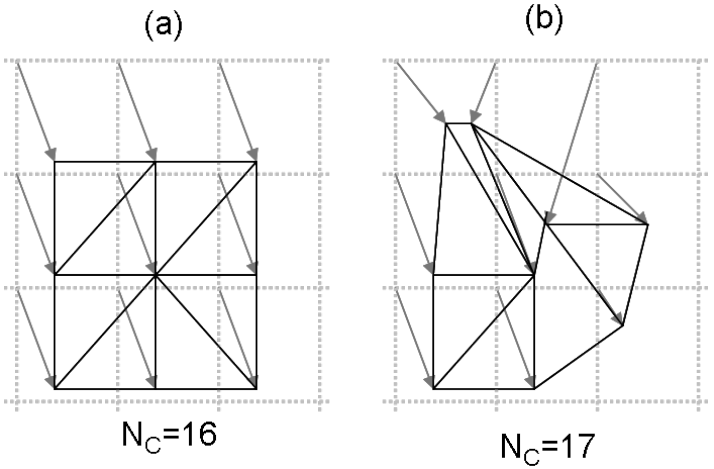

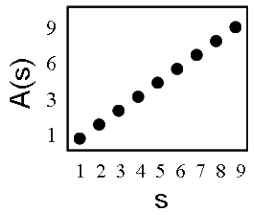

A(s)=[1,2,3,4,5,6,7,8.9]

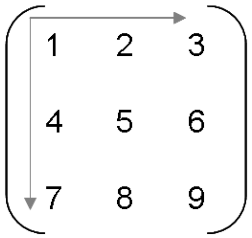

$$G_A = \frac{N_C - N_V}{N_V},$$

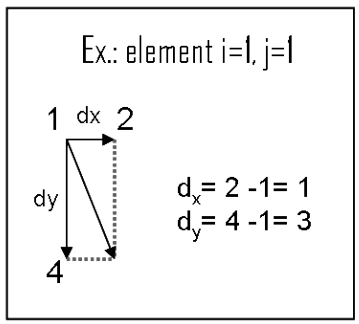

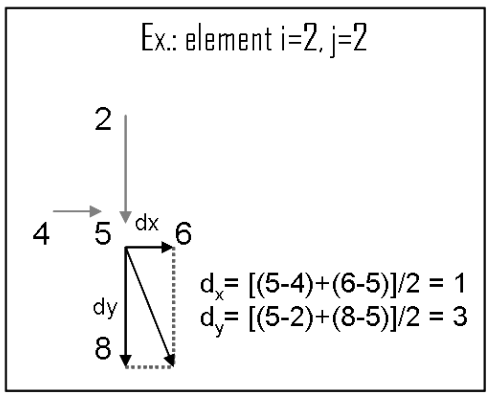

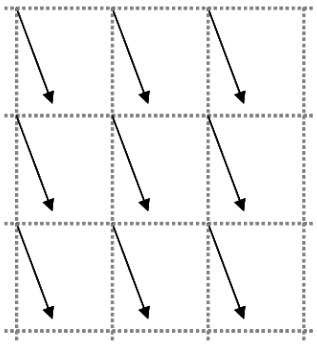

Ex.: Elementar ramp

GA=(16-9)/9=0.7777

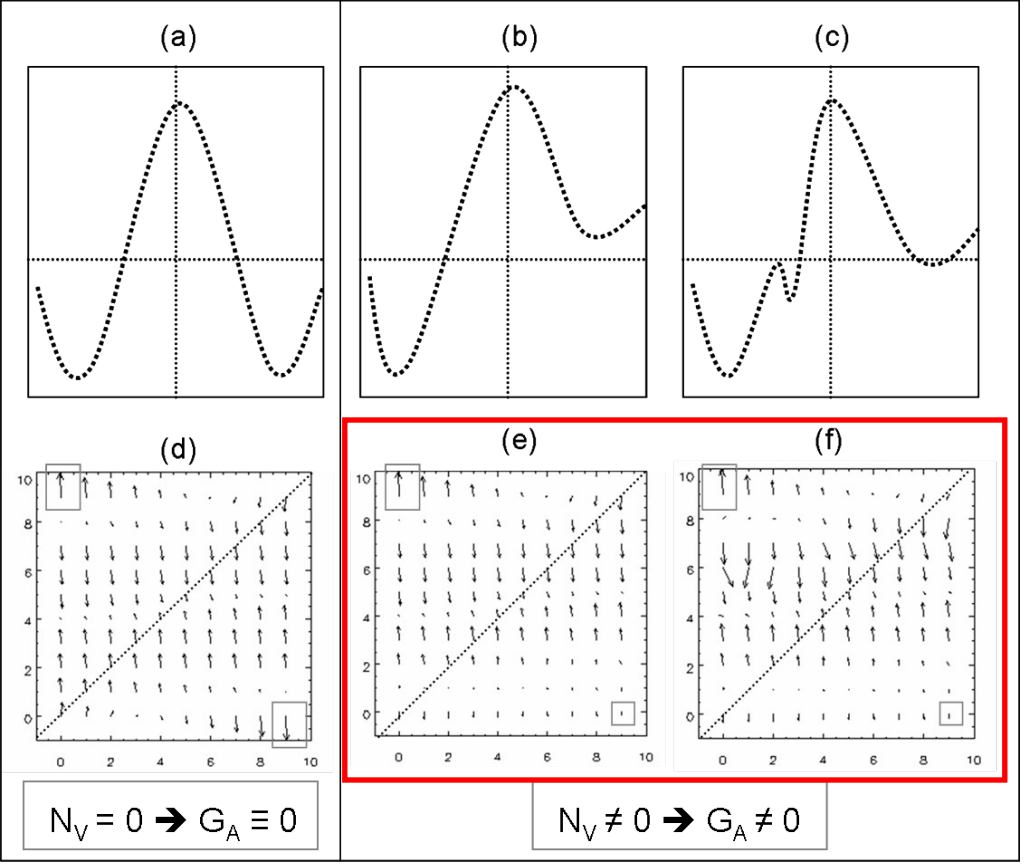

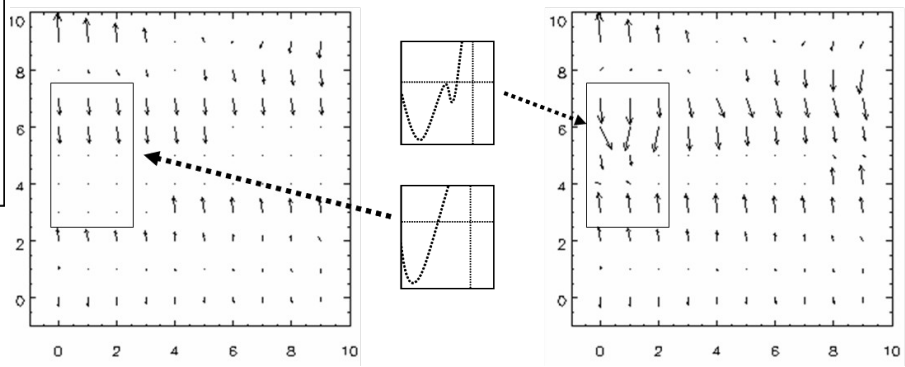

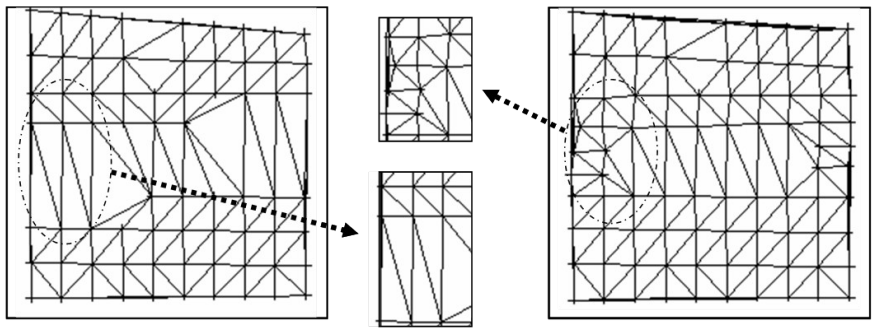

N_V=70, N_C=198, G_A=1.829

N_V=86, N_C=248, G_A=1.884

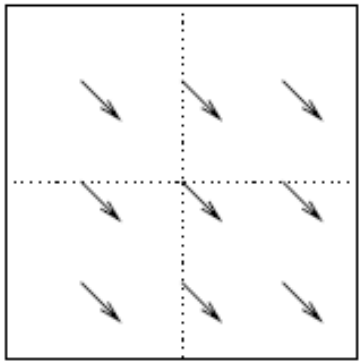

(a)

V= 9
L = 9

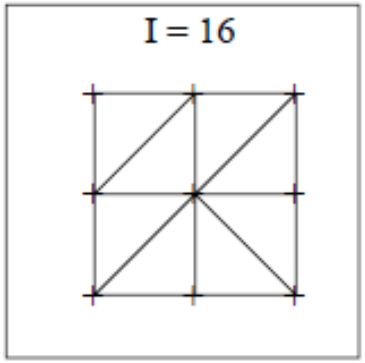

G_A=0.778

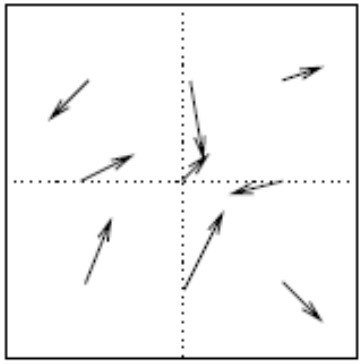

(b)

V= 9
L = 9

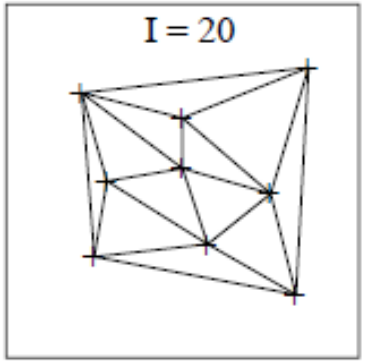

G_A=1.222

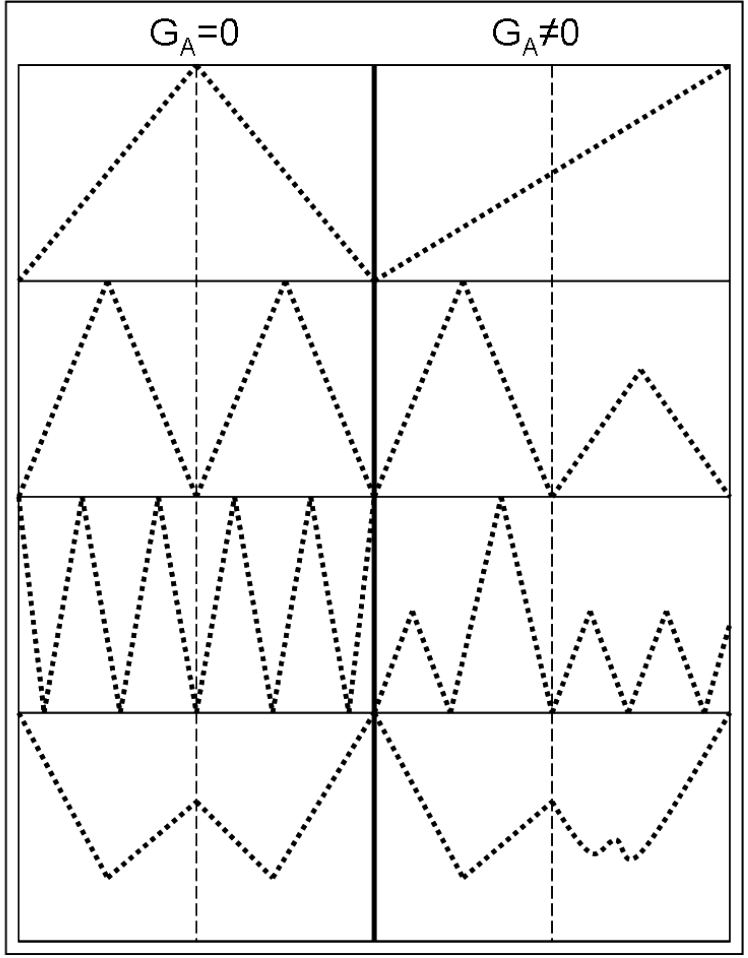

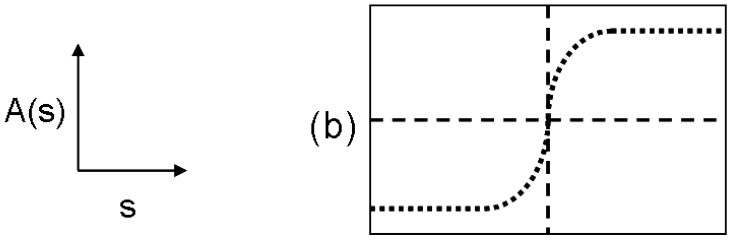

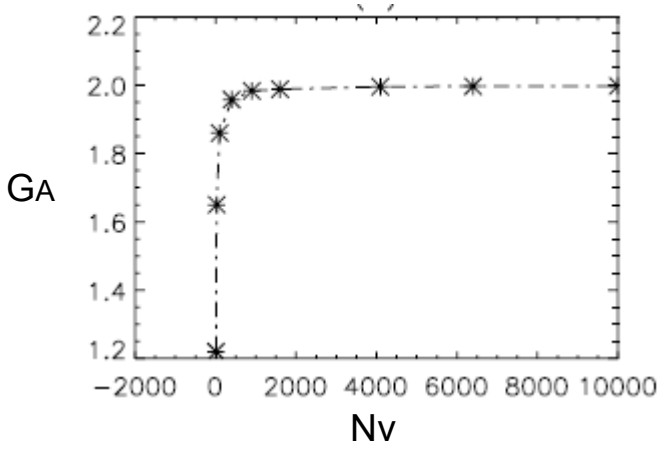

3×3	9	18	1.2200	0.2200
5×5	25	65	1.6500	0.1700
10×10	100	285	1.8600	0.0120
20×20	400	1186	1.9575	0.0076
30×30	900	2685	1.9833	0.0031
40×40	1600	4781	1.9881	0.0016
64×64	4096	12269	1.9954	0.0009
80×80	6400	19199	1.9968	0.0003
100×100	10000	29975	1.9974	0.0002
128×128	16384	49140	1.9992	0.0001

International Journal of Modern Physics C, Vol. 10, No. 1 (1999) 147–163
© World Scientific Publishing Company

CHARACTERIZATION OF ASYMMETRIC FRAGMENTATION PATTERNS IN SPATIALLY EXTENDED SYSTEMS

R. R. ROSA[*,‡,¶], A. S. SHARMA[†,§], and J. A. VALDIVIA[†]

[*]*Lab for Computing and Applied Mathematics (LAC)*
National Institute for Space Research-INPE, Brazil
Cx. Postal 515, 12201-970, S. J. dos Campos, SP, Brazil
[‡]*E-mail: reinaldo@lac.inpe.br*

[†]*Astronomy and Physics Departments, University of Maryland*
College Park-MD, 20742-2421, USA
[§]*E-mail: ssh@avl.umd.edu*

In this case, the difference $(I - L)$ will increase with L as follows:

$$\lim_{L\to\infty} (I - L) \simeq 2L. \tag{1}$$

Therefore, given a $n \times n$ size matrix, for which $L \approx n^2$, the $(I-L)/L$ ratio for a big n, tends to 2. This asymptotic regime implies a very high accuracy of the value $(I - L)/L$ to compare different matrices of the same size for $L > 100$.

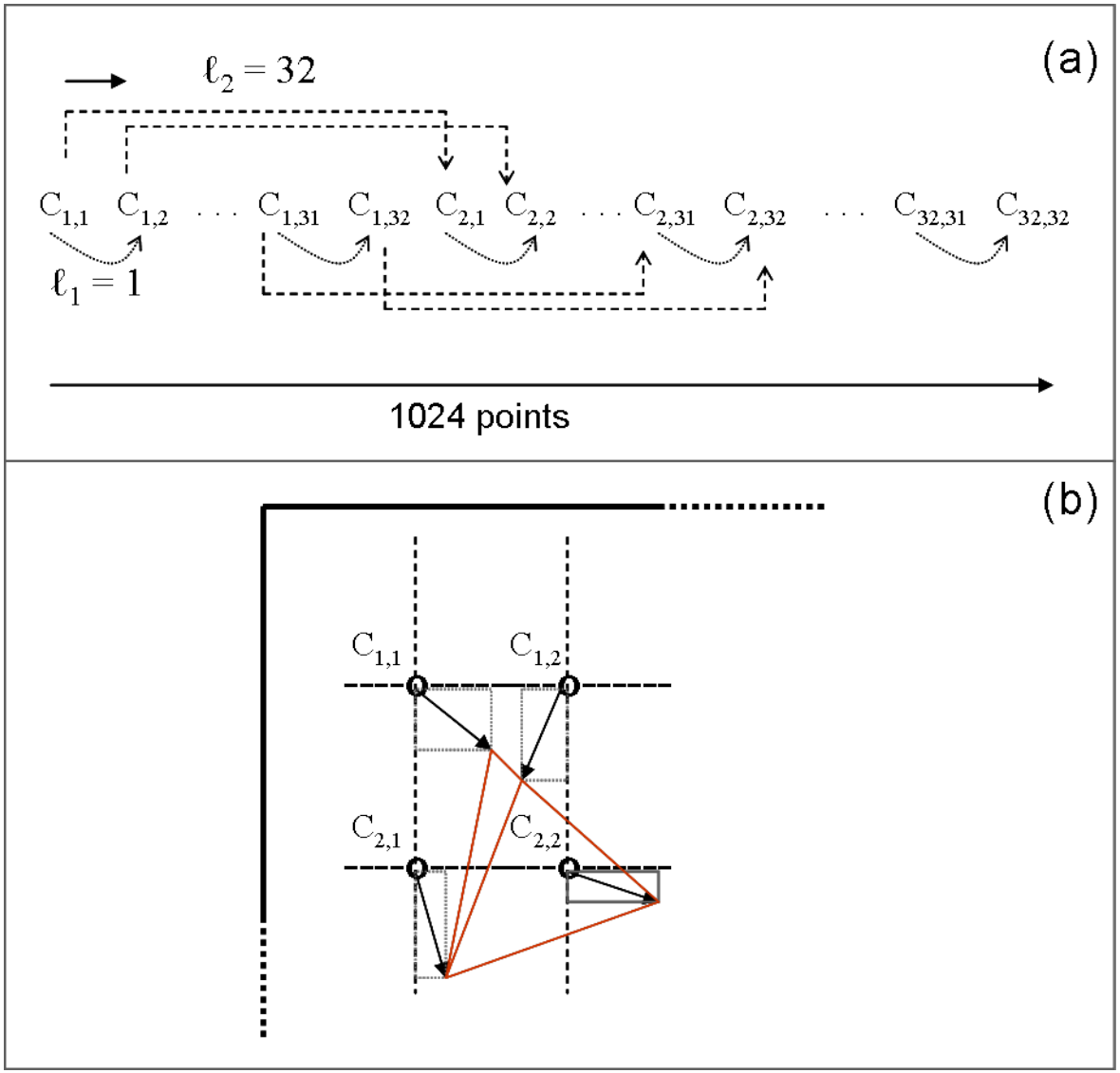
(a)
$\ell_2 = 32$
$C_{1,1}$ $C_{1,2}$ . . . $C_{1,31}$ $C_{1,32}$ $C_{2,1}$ $C_{2,2}$ . . . $C_{2,31}$ $C_{2,32}$ . . . $C_{32,31}$ $C_{32,32}$
$\ell_1 = 1$
1024 points
(b)
$C_{1,1}$
$C_{1,2}$
$C_{2,1}$
$C_{2,2}$

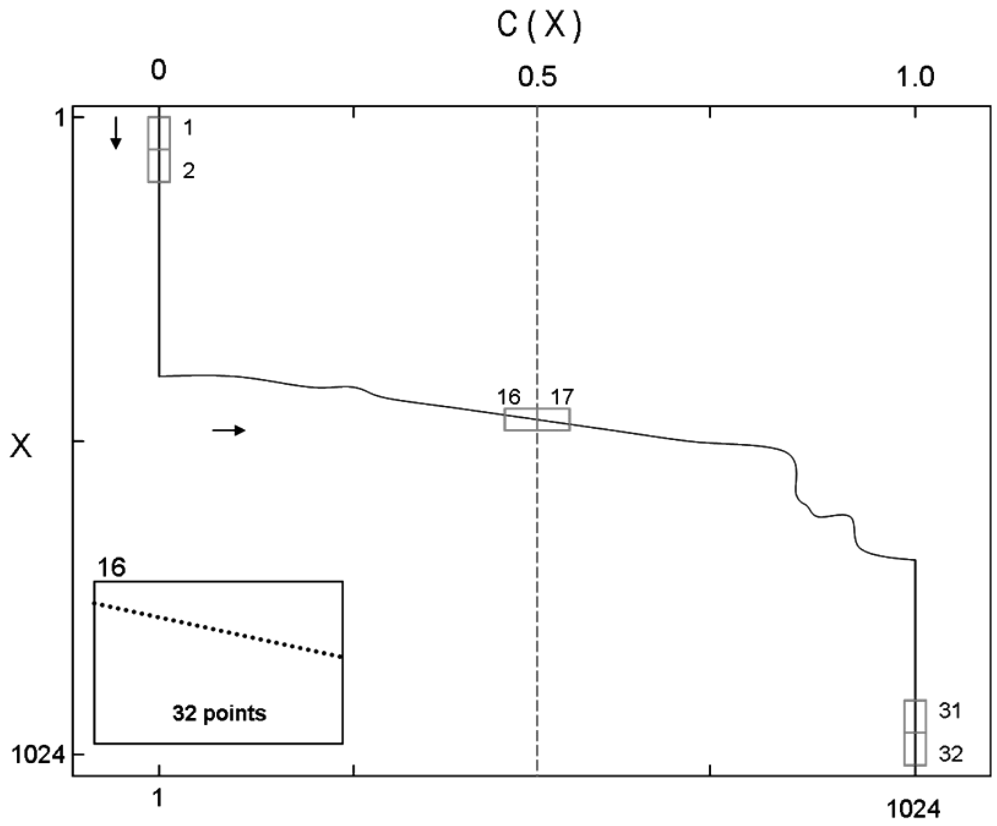

(a)

$$
\begin{array}{c|c}
1 & C_{1,1}\ C_{1,2}\ C_{1,3}\ \ldots\ C_{1,31}\ C_{1,32} \\
2 & C_{2,1}\ C_{2,2}\ C_{2,3}\ \ldots\ C_{2,31}\ C_{2,32} \\
\vdots & \vdots \\
16 & C_{16,1}\ C_{16,2}\ C_{16,3}\ \ldots\ C_{16,32}\ C_{16,32} \\
17 & C_{17,1}\ C_{17,2}\ C_{17,3}\ \ldots\ C_{17,31}\ C_{17,32} \\
\vdots & \vdots \\
31 & C_{31,1}\ C_{31,2}\ C_{31,3}\ \ldots\ C_{31,31}\ C_{31,32} \\
32 & C_{32,1}\ C_{32,2}\ C_{32,3}\ \ldots\ C_{32,31}\ C_{32,32}
\end{array}
$$

(b)

t=0

t

t=1000

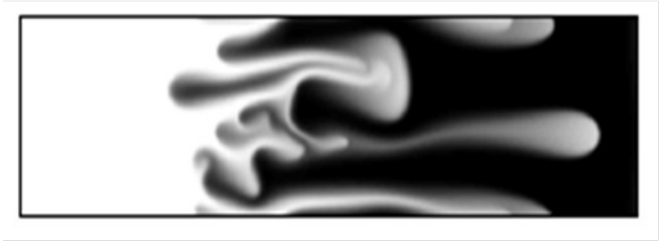

t=2000

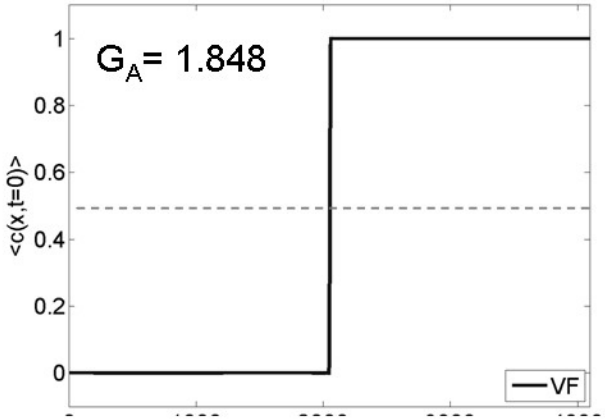

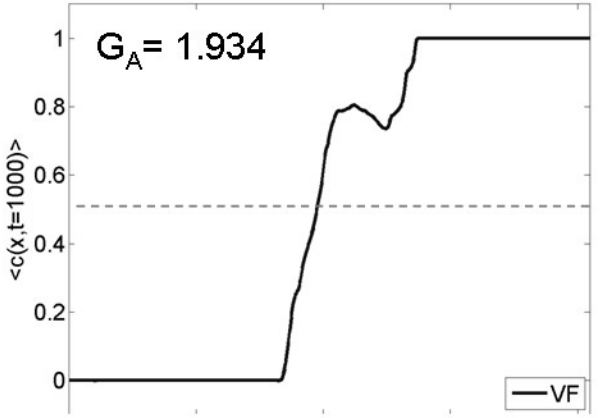

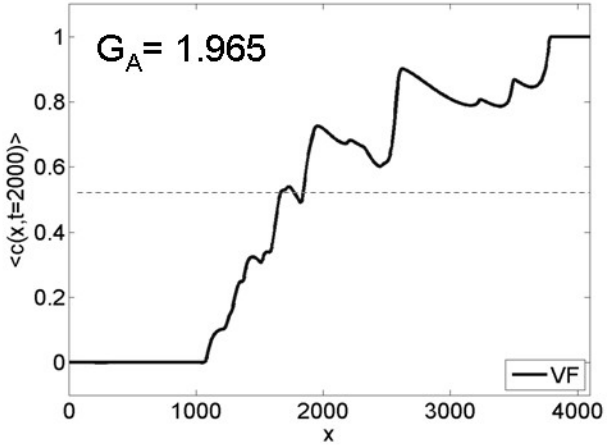

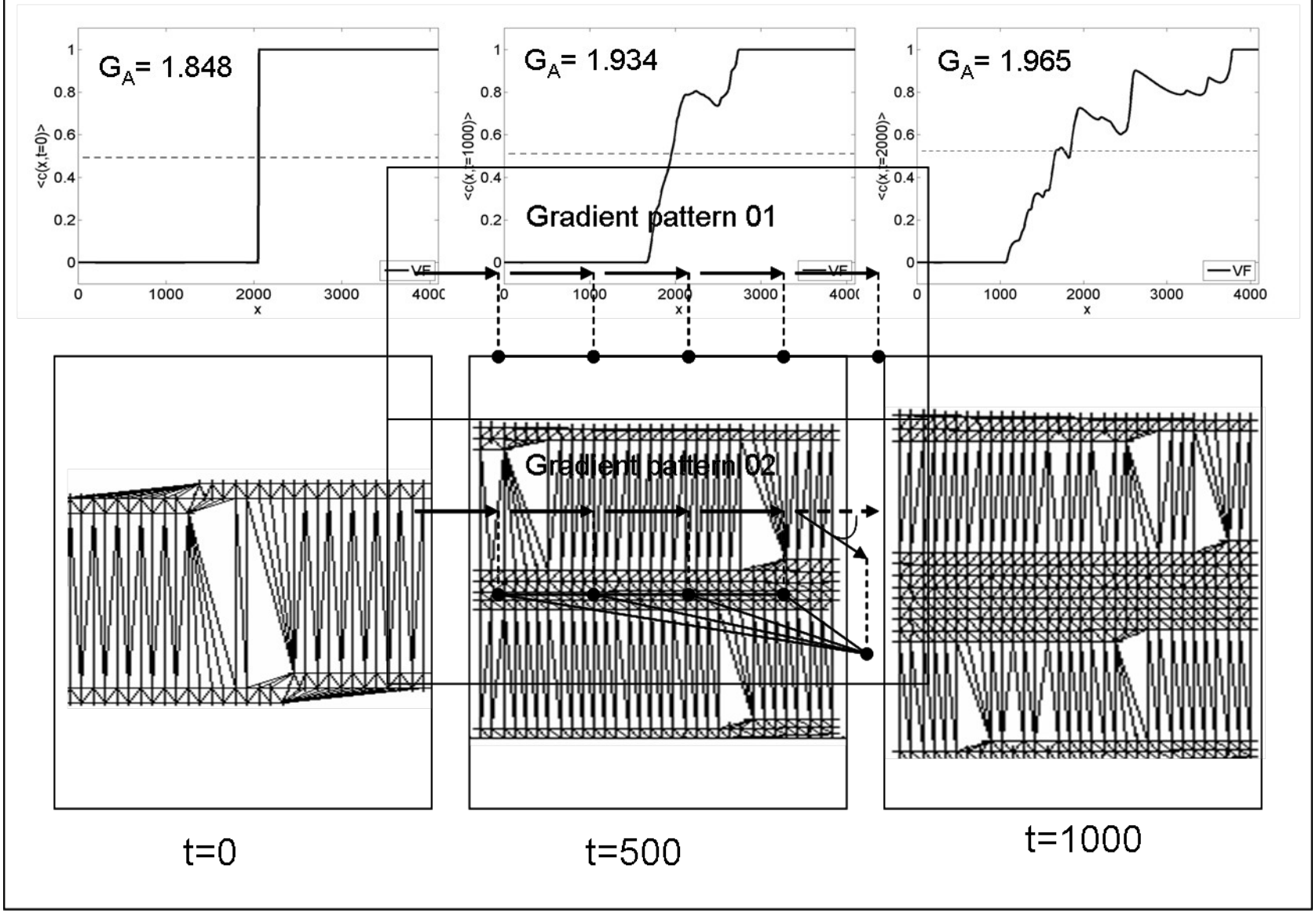
G_A= 1.848
G_A= 1.934
G_A= 1.965
<c(x,t=0)>
<c(x,t=1000)>
<c(x,t=2000)>
x
VF
Gradient pattern 01
Gradient pattern 02
t=0
t=500
t=1000

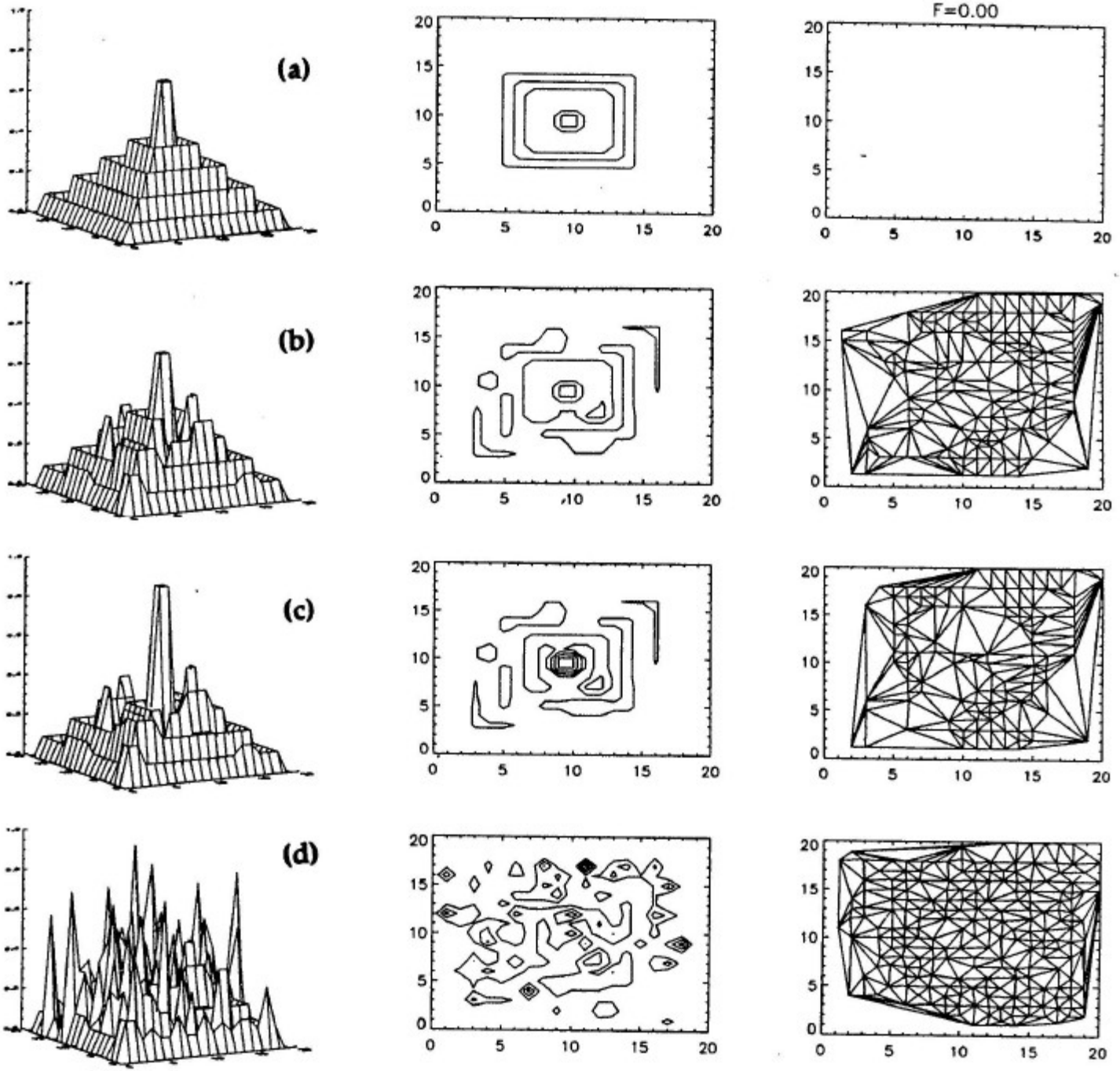
(a)
(b)
(c)
(d)
F=0.00

Z = 0

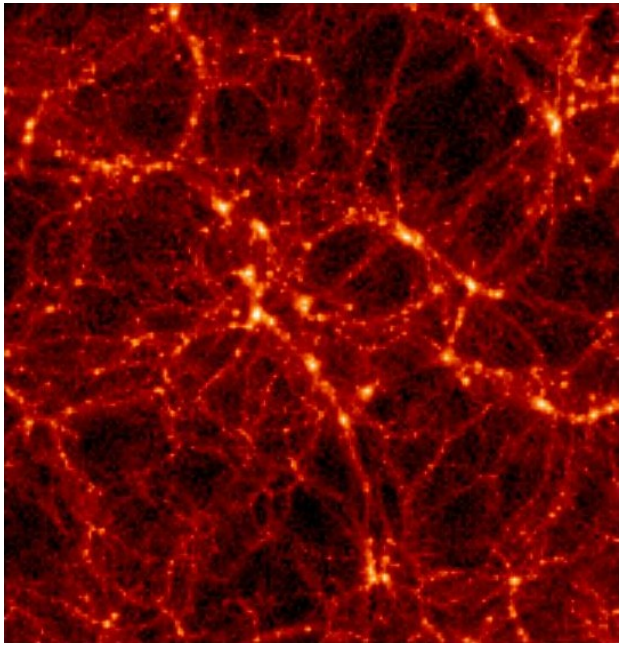

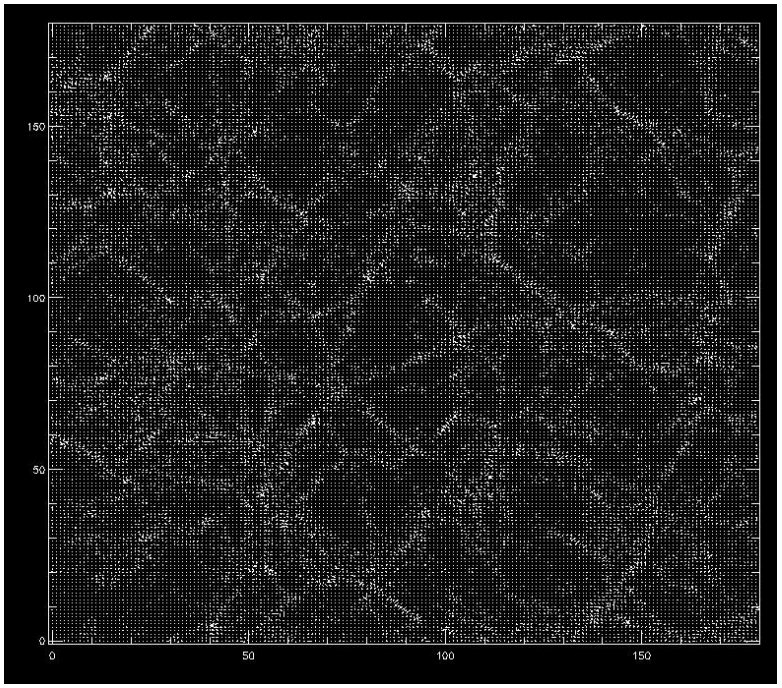

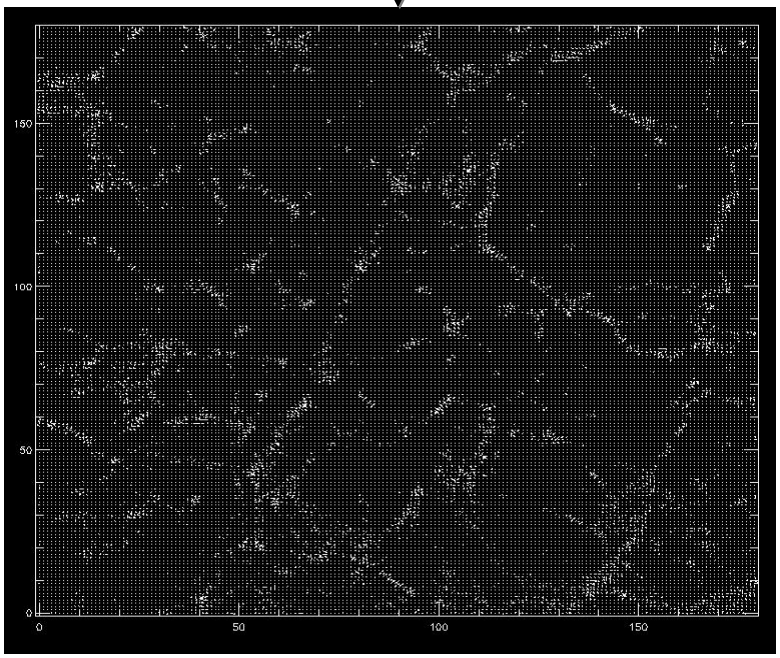

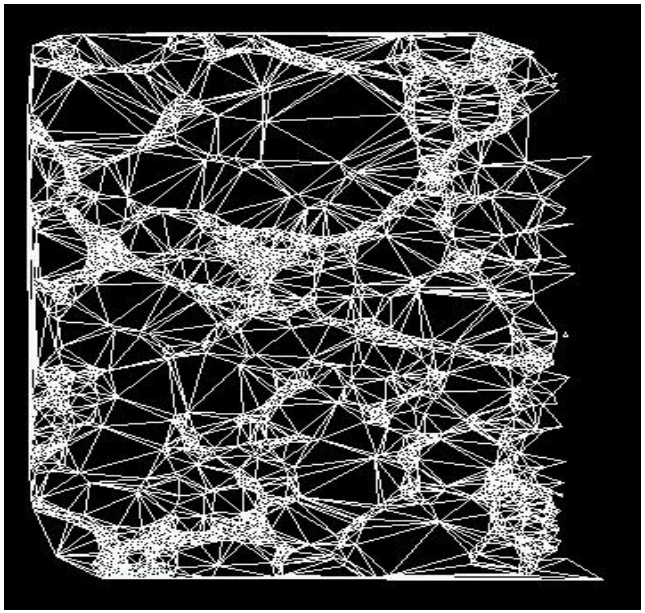

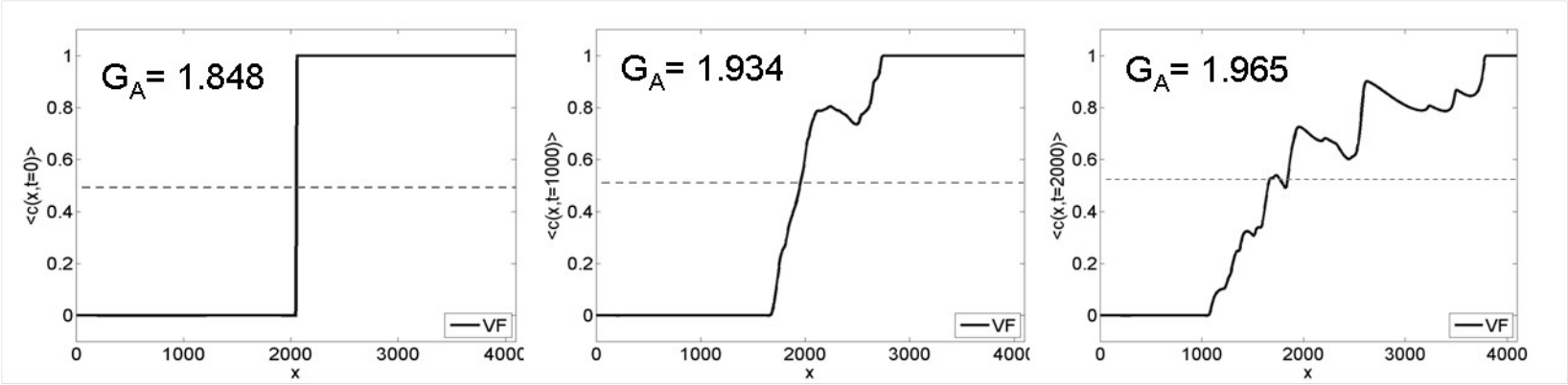

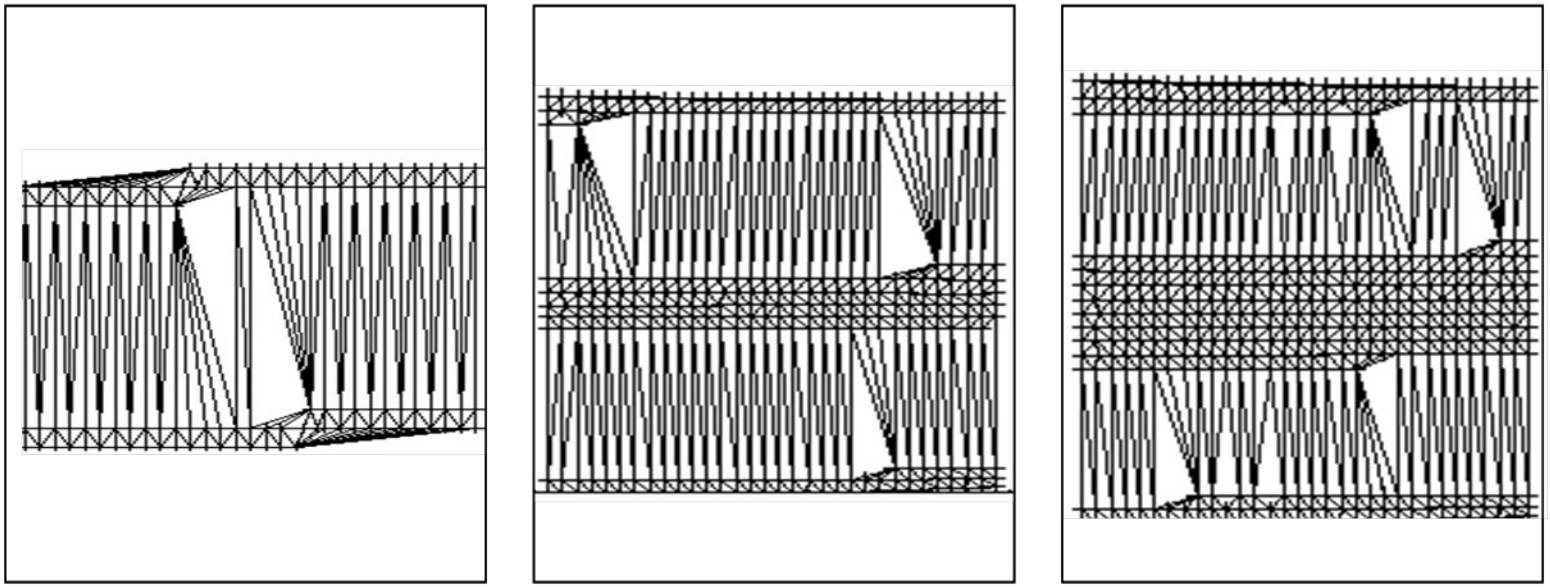

t=0 t=500 t=1000

RESULTS

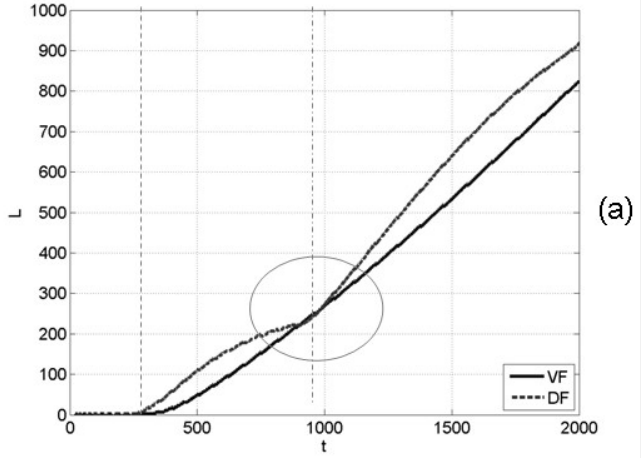

(a)

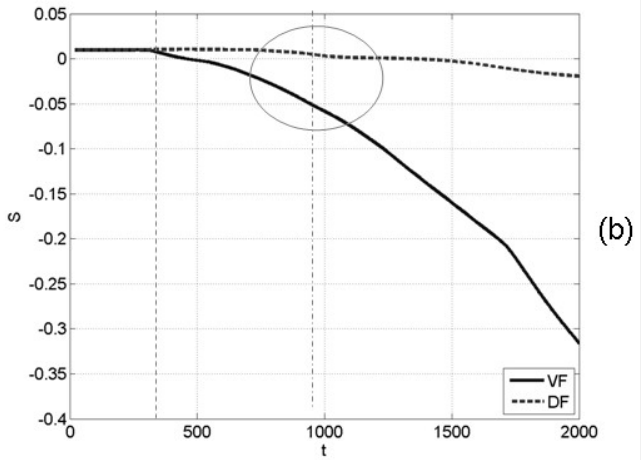

(b)

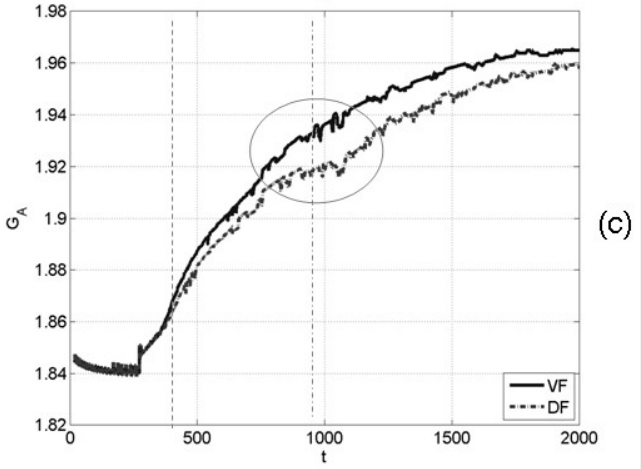

(c)

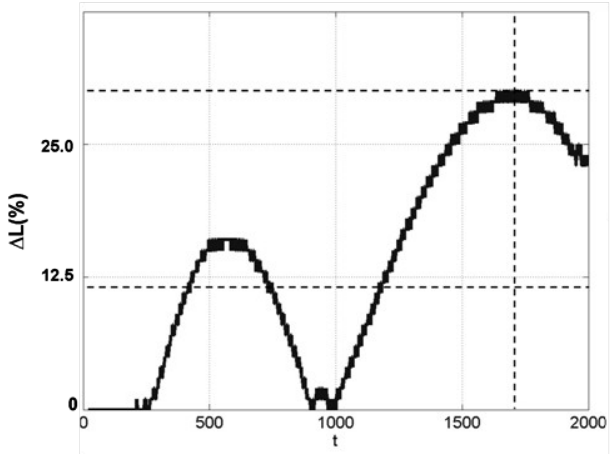

(d)

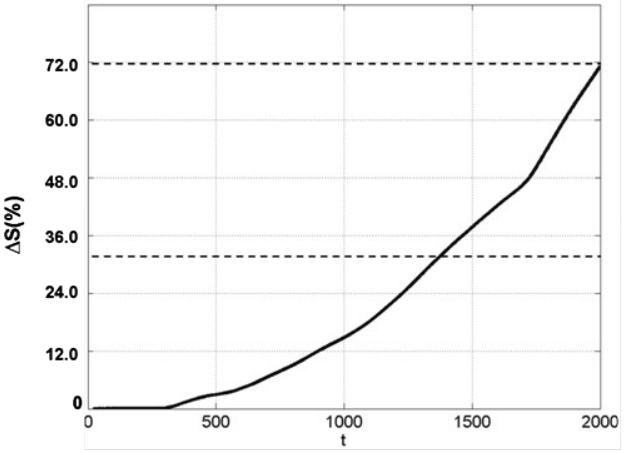

(e)

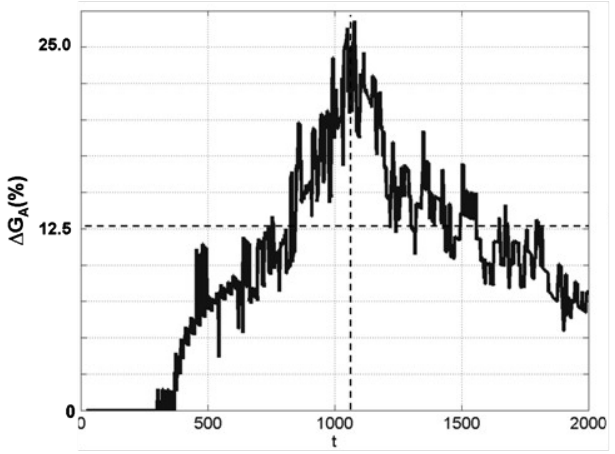

(f)

Table I: Average and standard deviation of asymmetry coefficient for transversely concentration profiles composed by 1024 points.

t	$\overline{G_A} \pm \Delta G_A$ (VF)	$\overline{G_A} \pm \Delta G_A$ (DF)
500	1.885 ± 0.001	1.881 ± 0.001
1000	1.935 ± 0.002	1.919 ± 0.002
1500	1.960 ± 0.002	1.946 ± 0.002
2000	1.968 ± 0.003	1.956 ± 0.003

Table II: Structural comparative analysis between density and viscous fingerings.

μ	$t_{0,d}(\%)$	$\overline{\mu}_{DF}/\overline{\mu}_{VF}$	$\overline{\Delta\mu}(\%)$	$\Delta\mu_{max}(\%)(t)$	$FineStructures$	MPPD
L	13.4	1.18	12.2	30.5(1700)	Low	mixing
S	13.5	1.83	32.5	72.0(2000)	None	nonlinear coarsening
G_A	15.5	0.98	12.5	26.5(1088)	High	side-finger instability

APPLICATION 1: Space Physics

$$R_a = \frac{\Delta \rho g \kappa L_h}{\nu D}$$

Planeta	$g\ (m/s^2)$	R_a	R_a	R_a
Terra	9,7660	1	2	3
Mercurio	3,7000	0,37887	0,75773	1,13660
Vênus	8,8700	0,90825	1,81651	2,72476
Marte	3,6930	0,37815	0,75630	1,13445
Jupiter	20,8700	2,13701	4,27401	6,41102
Saturno	10,4000	1,06492	2,12984	3,19476
Urano	8,4300	0,86320	1,72640	2,58960
Netuno	10,7100	1,09666	2,19332	3,28999
Plutão	0,8100	0,08294	0,16588	0,24882
Lua (satélite natural da Terra)	1,6220	0,16609	0,33217	0,49826

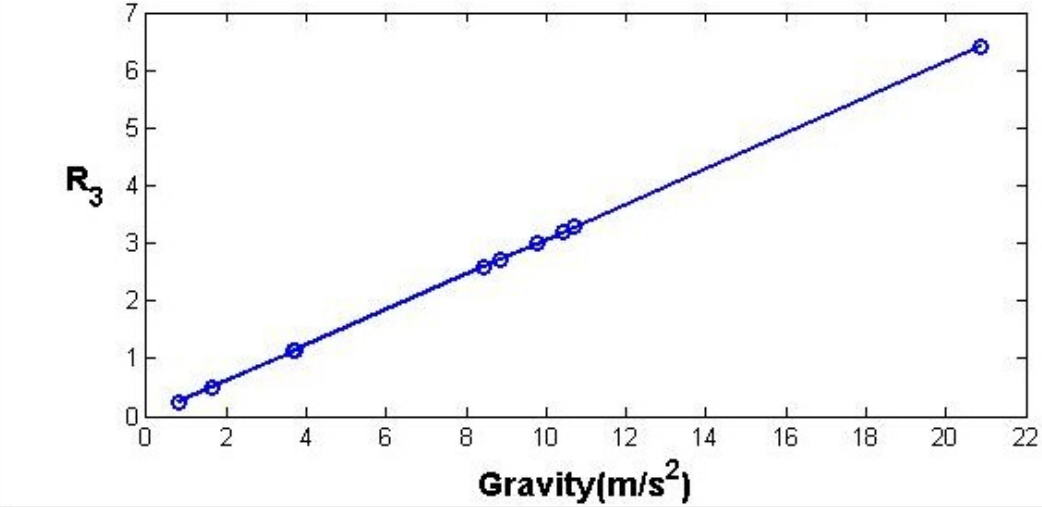

Pluto (0,8;0,25)

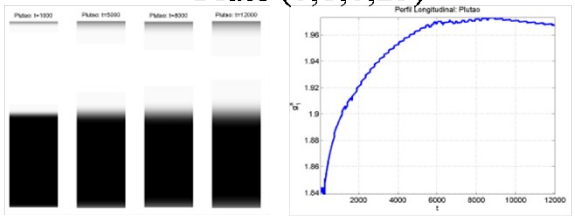

Venus (8,87;2,72)

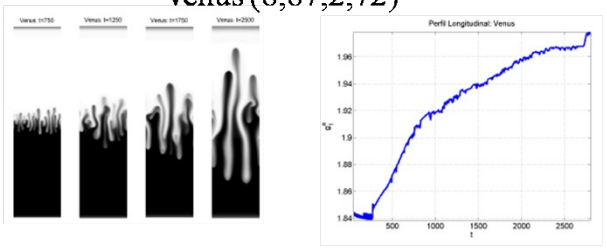

Moon (1,6;0,50)

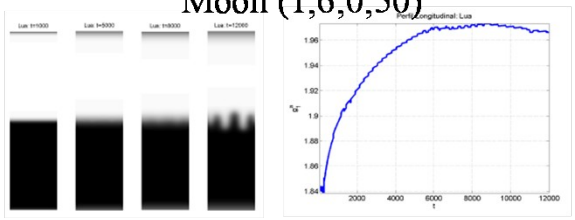

Terra (9,8,;3)

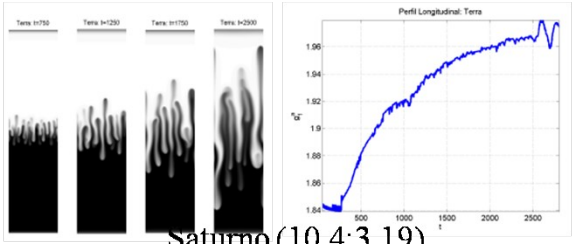

Mars (3,69;1,13)

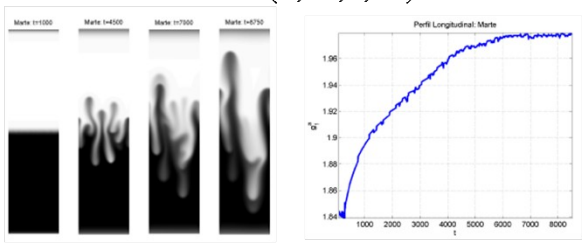

Saturno (10,4;3,19)

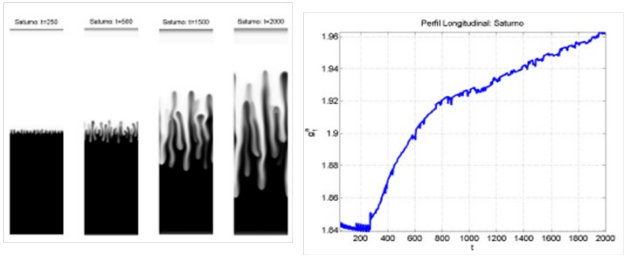

Mercury (3,7;1,14)

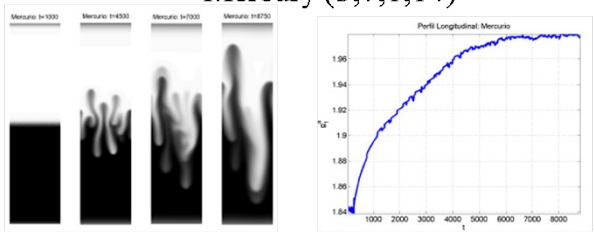

Netune (10,7;3,28)

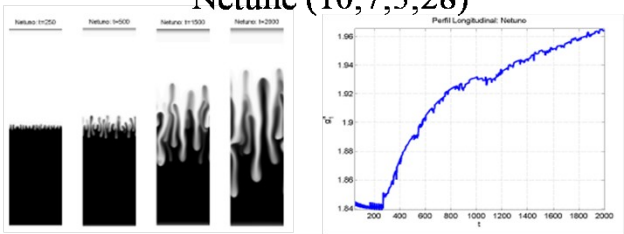

Urane (8,43;2,6)

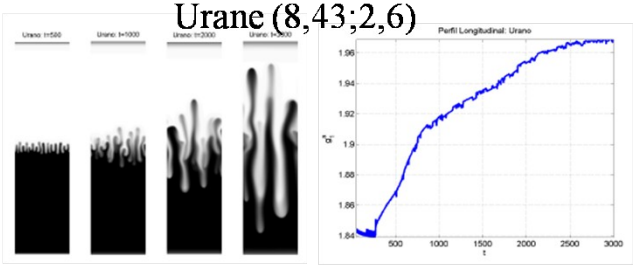

Jupiter (20,9;6,41)

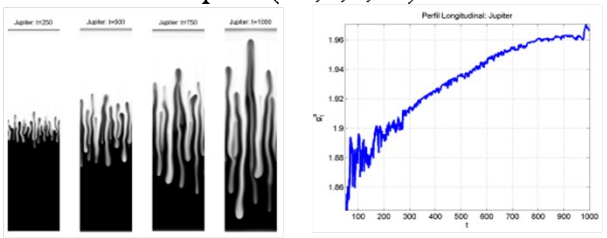

APPLICATION 2: Environmental Sciences

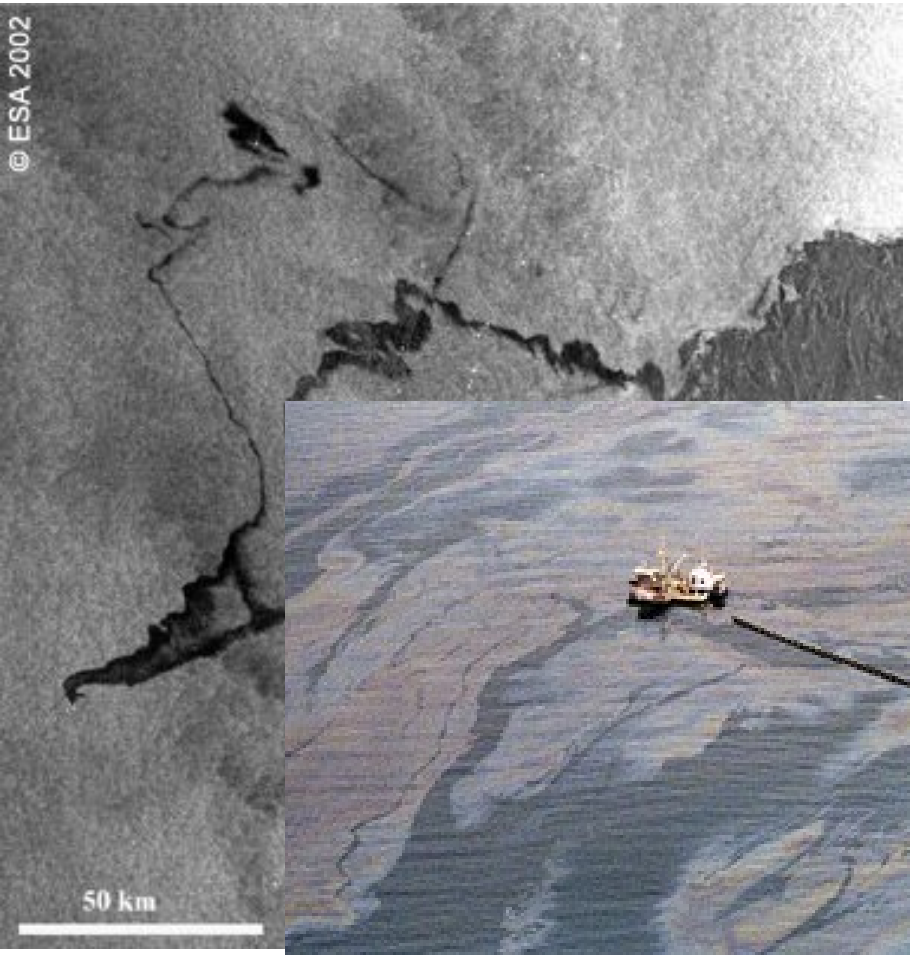

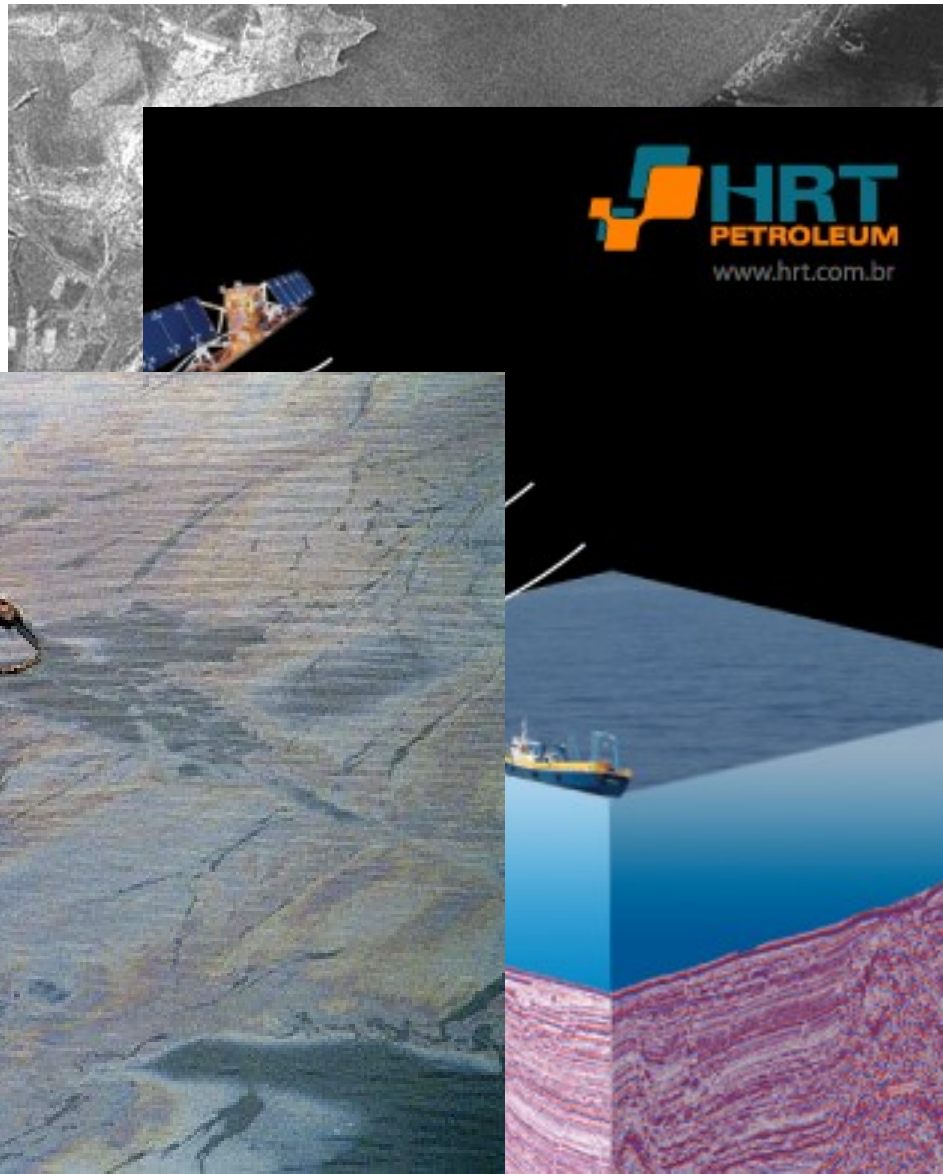

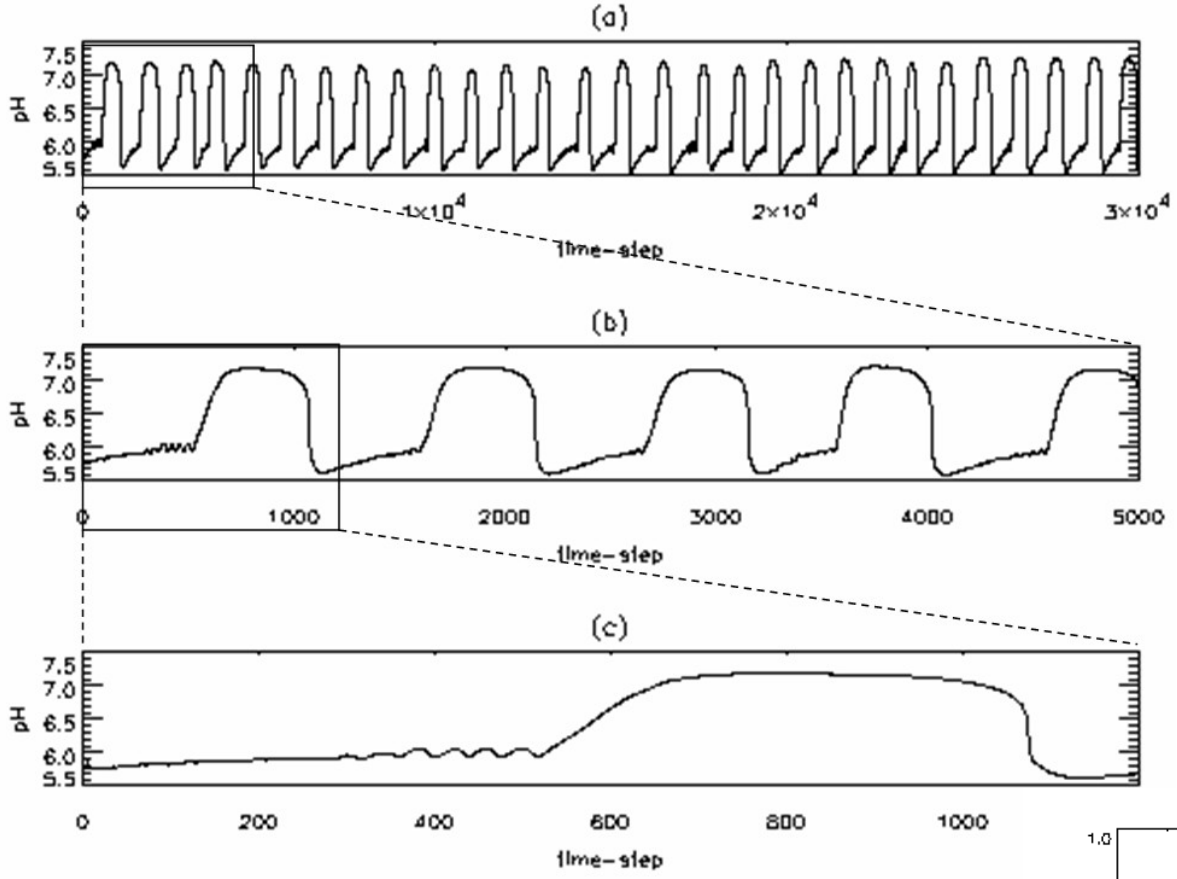

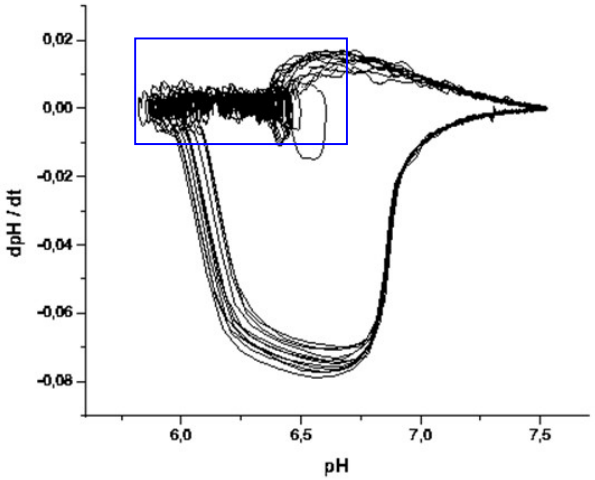

Fig. 1. Bursting oscillations observed in the hemin - hydrogen peroxide – sulfite reaction system.

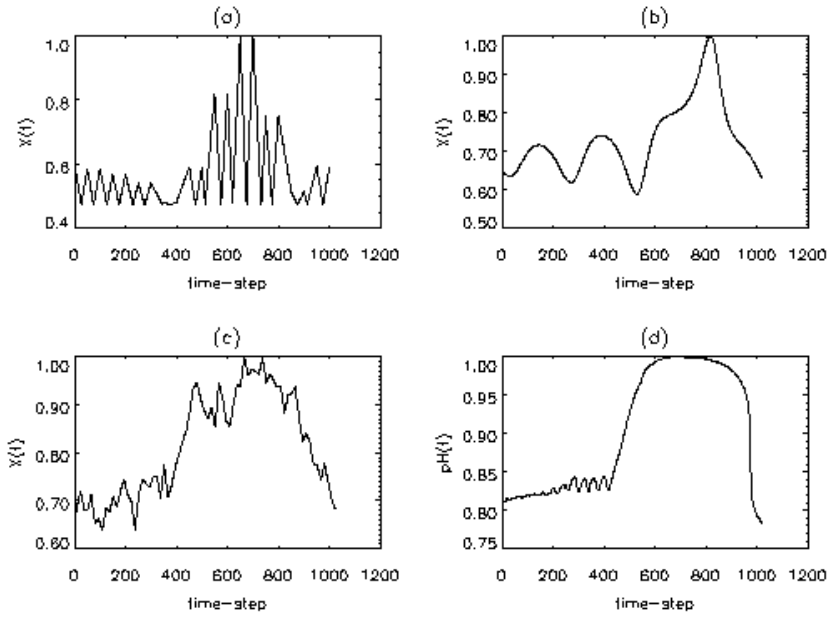

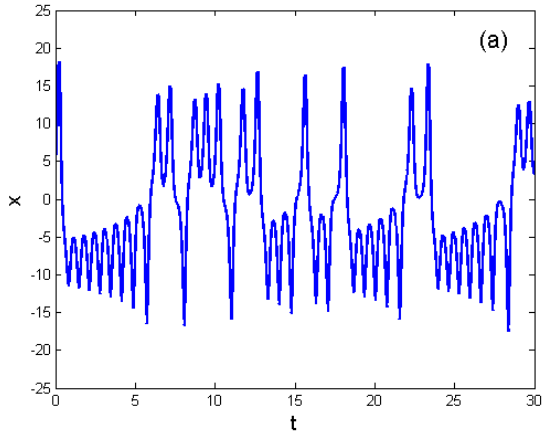
(a)
x
t

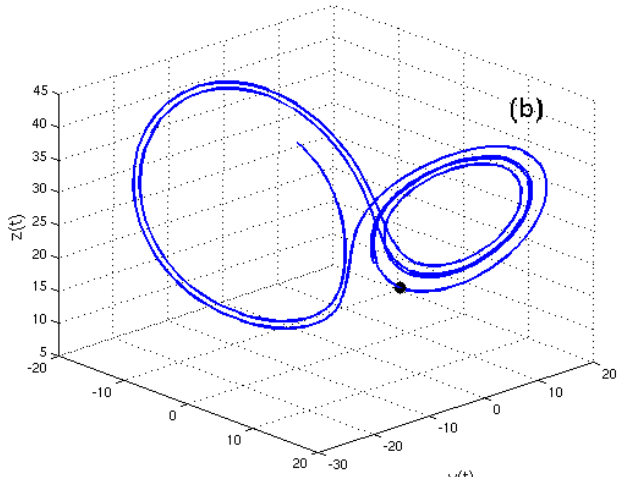
(b)
z(t)

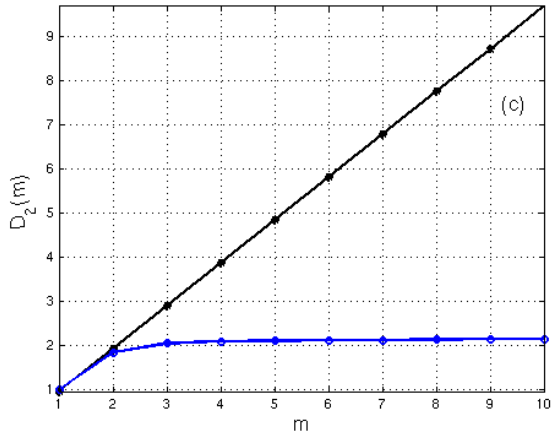
(c)
D2(m)
m

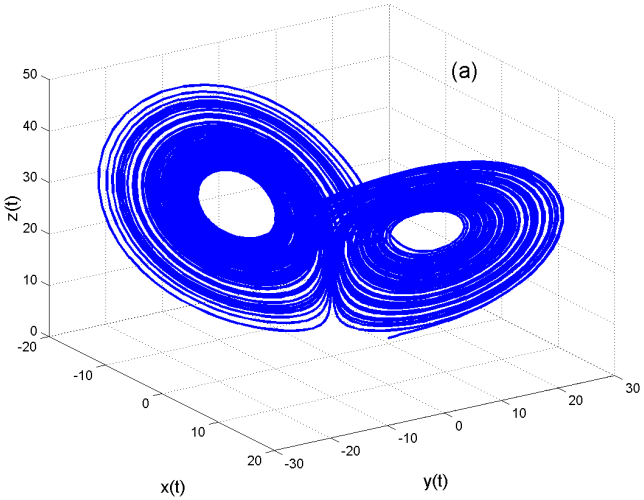
(a)
z(t)
x(t)
y(t)

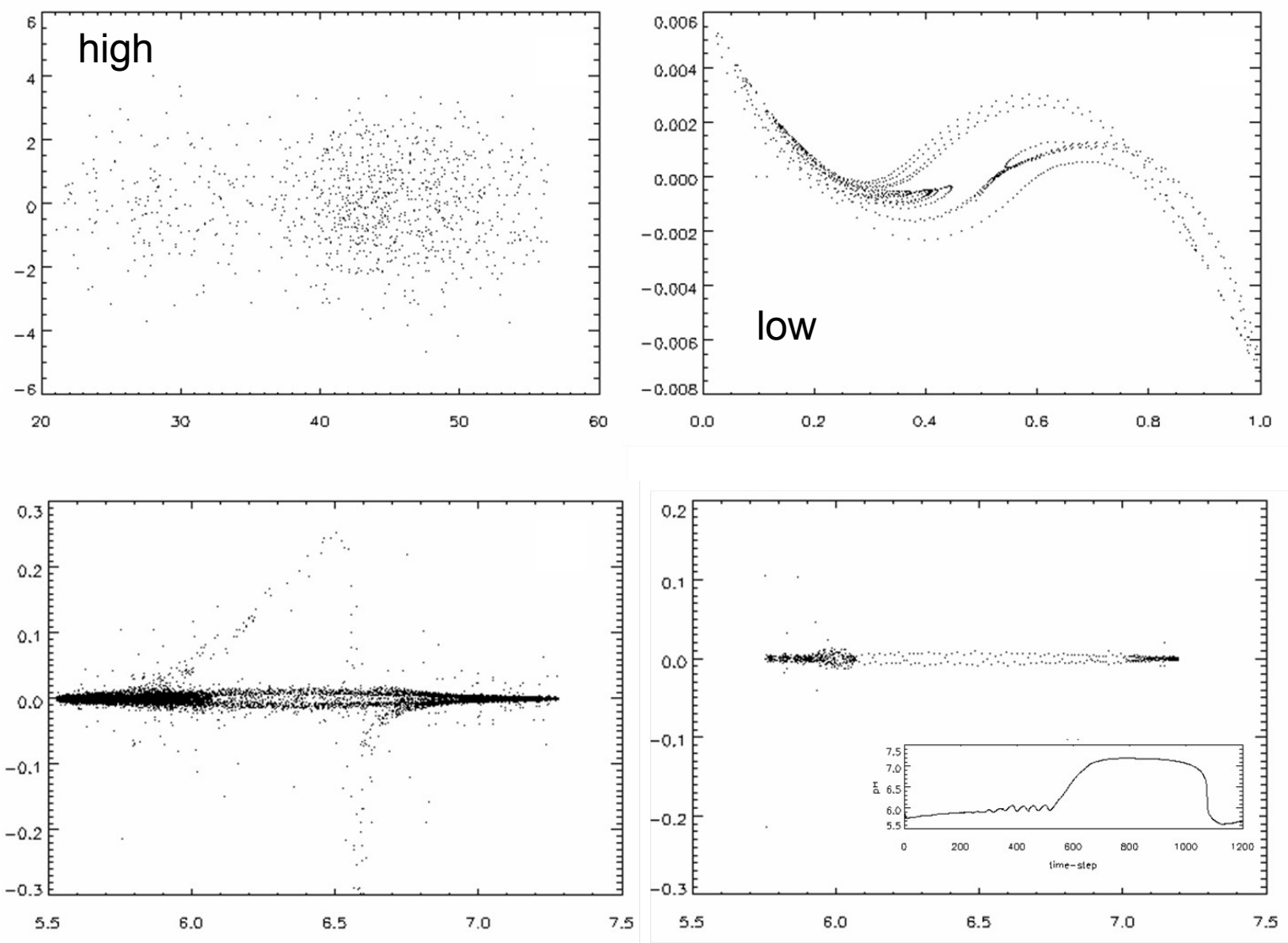
high
low
pH
time-step

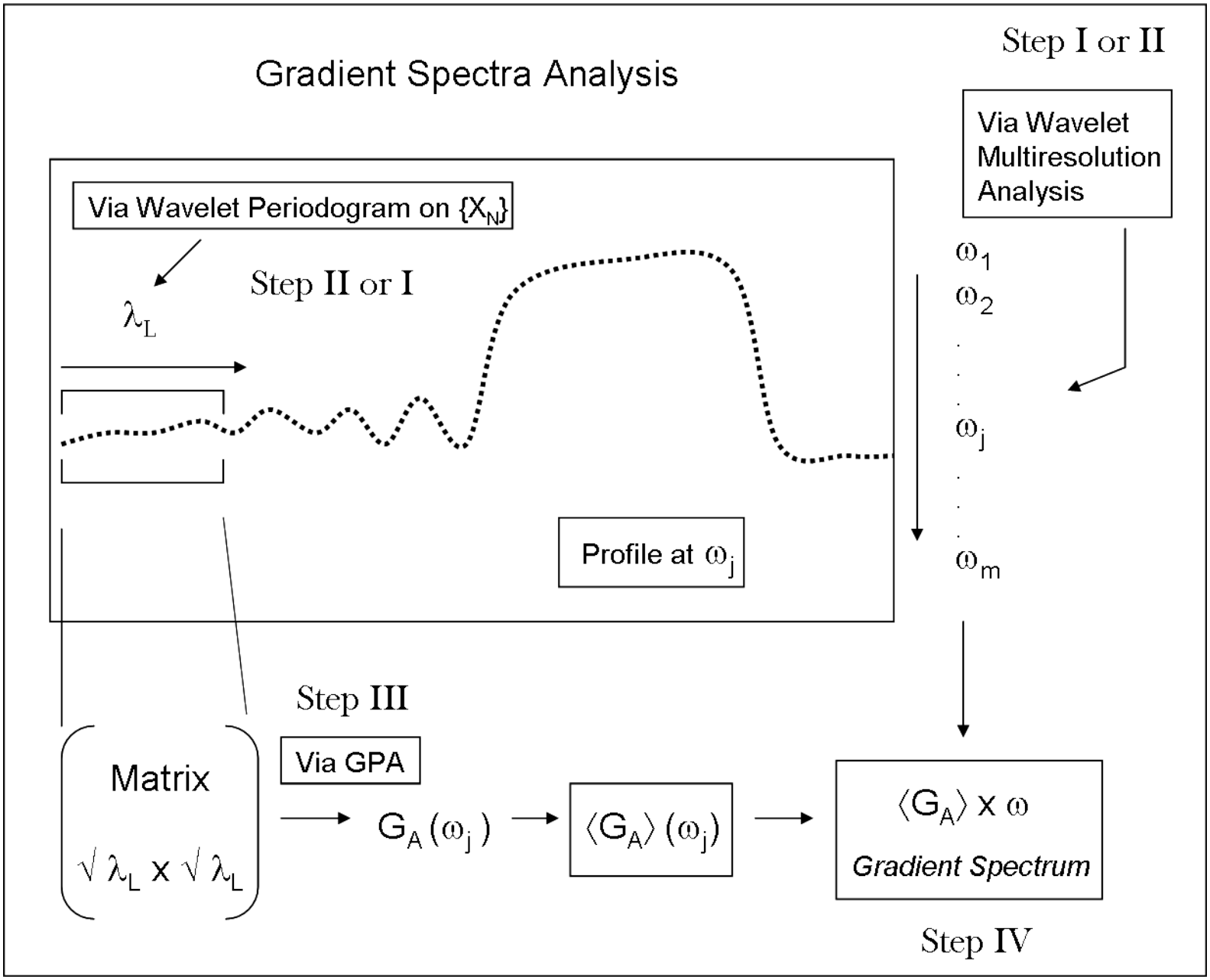
Gradient Spectra Analysis
Step I or II
Via Wavelet Multiresolution Analysis
Via Wavelet Periodogram on {X_N}
Step II or I
λ_L
ω_1
ω_2
ω_j
ω_m
Profile at ω_j
Step III
Via GPA
Matrix
√λ_L x √λ_L
G_A(ω_j)
⟨G_A⟩(ω_j)
⟨G_A⟩ x ω
Gradient Spectrum
Step IV

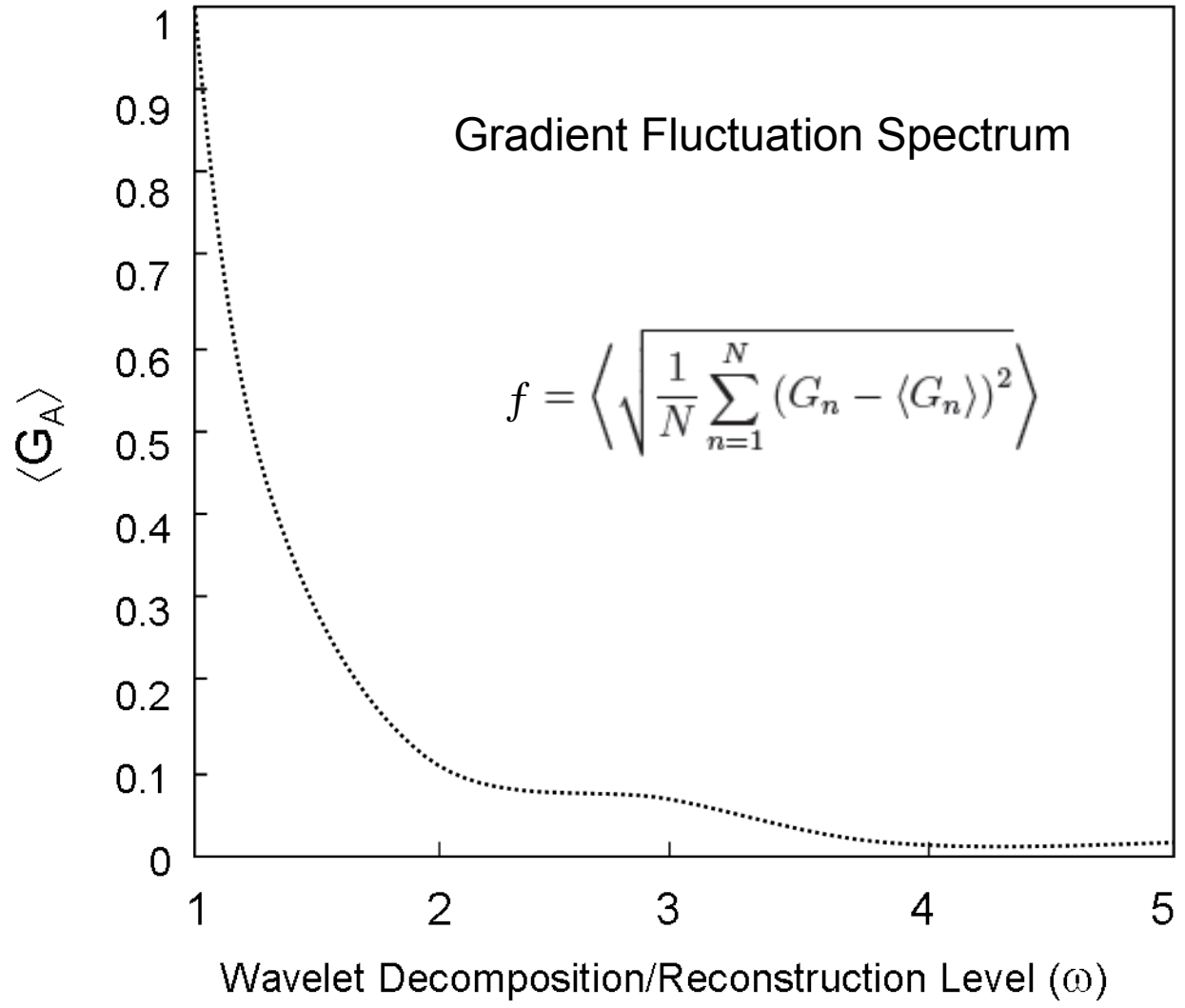
Gradient Fluctuation Spectrum
$f = \left\langle \sqrt{\frac{1}{N}\sum_{n=1}^{N}(G_n - \langle G_n \rangle)^2} \right\rangle$
$\langle G_A \rangle$
1
0.9
0.8
0.7
0.6
0.5
0.4
0.3
0.2
0.1
0
1
2
3
4
5
Wavelet Decomposition/Reconstruction Level (ω)

Characteristics measures for canonical time series and SAB.

Time-series	D	α	$\langle \bar{f} \rangle_{N=1024}$
Logistic	1	anti-persistent	0.940 ± 0.005
Kuramoto-Sivashinsky	1	anti-persistent	0.902 ± 0.005
H'enon	2	anti-persistent	0.865 ± 0.005
Lorenz	3	anti-persistent	0.800 ± 0.005
fB$\left[1/\omega^{1.5}\right]$	$\gg 6$	1.50	0.720 ± 0.002
fB$\left[1/\omega^{5/3}\right]$	$\gg 6$	1.66	0.650 ± 0.002
fB$\left[1/\omega^{2}\right]$	$\gg 6$	2.00	0.582 ± 0.002
SAB pH	?	?	0.830 ± 0.001

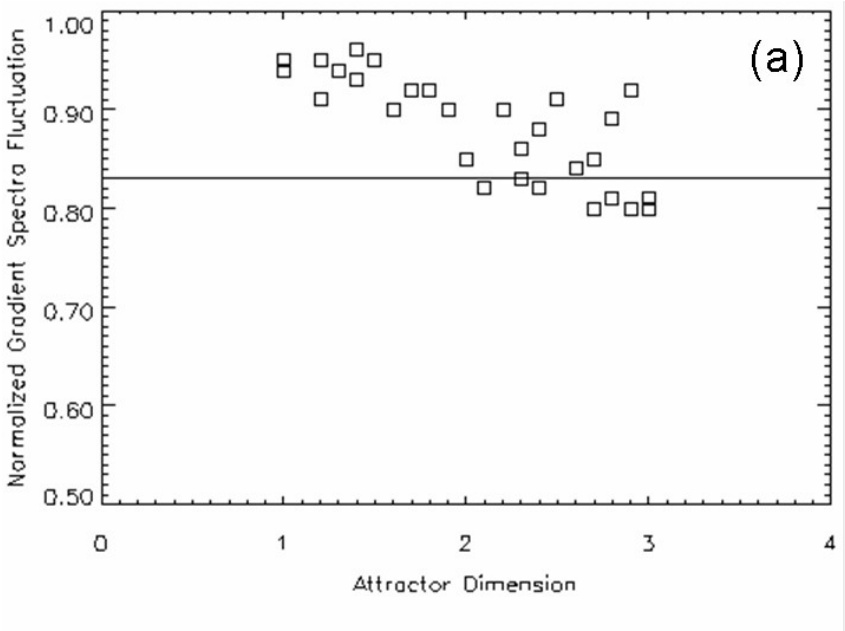

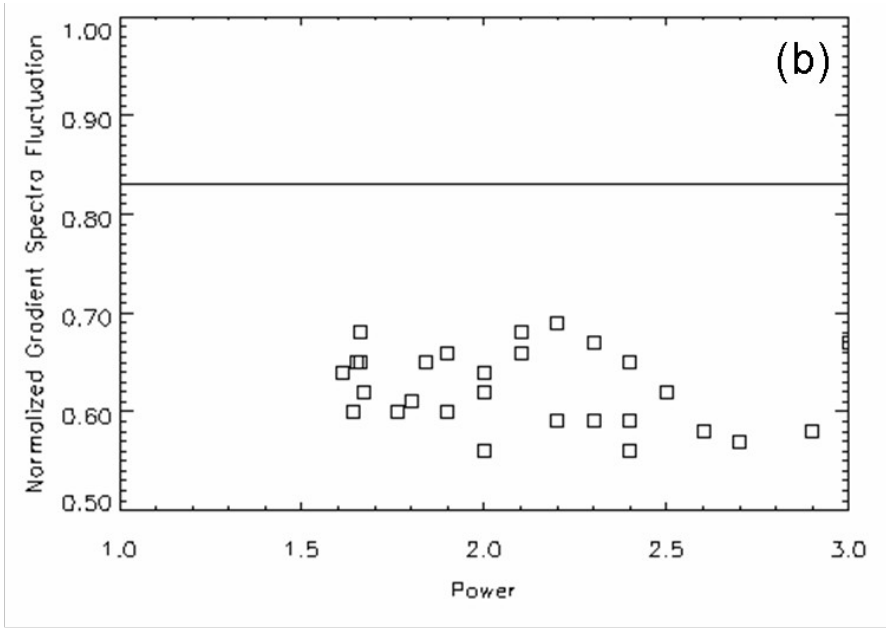

CCIS 2010

Conference
of Computational
Interdisciplinary
Sciences

S.J.Campos-Brazil
August 2010

http://epacis.org/

http://www.lac.inpe.br/CCIS

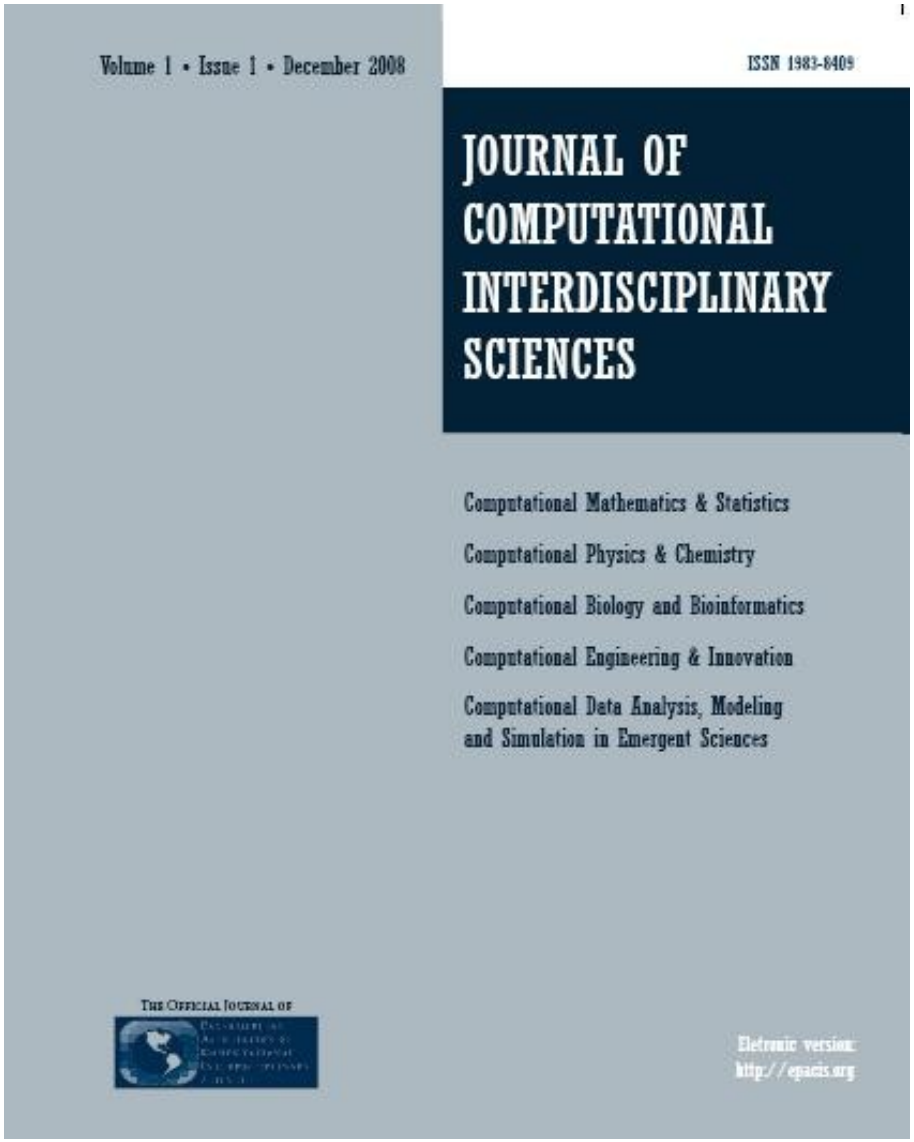

ISSN 1983-8409

GRADIENT PATTERN ANALISYS IN STRUCTURE FORMATION

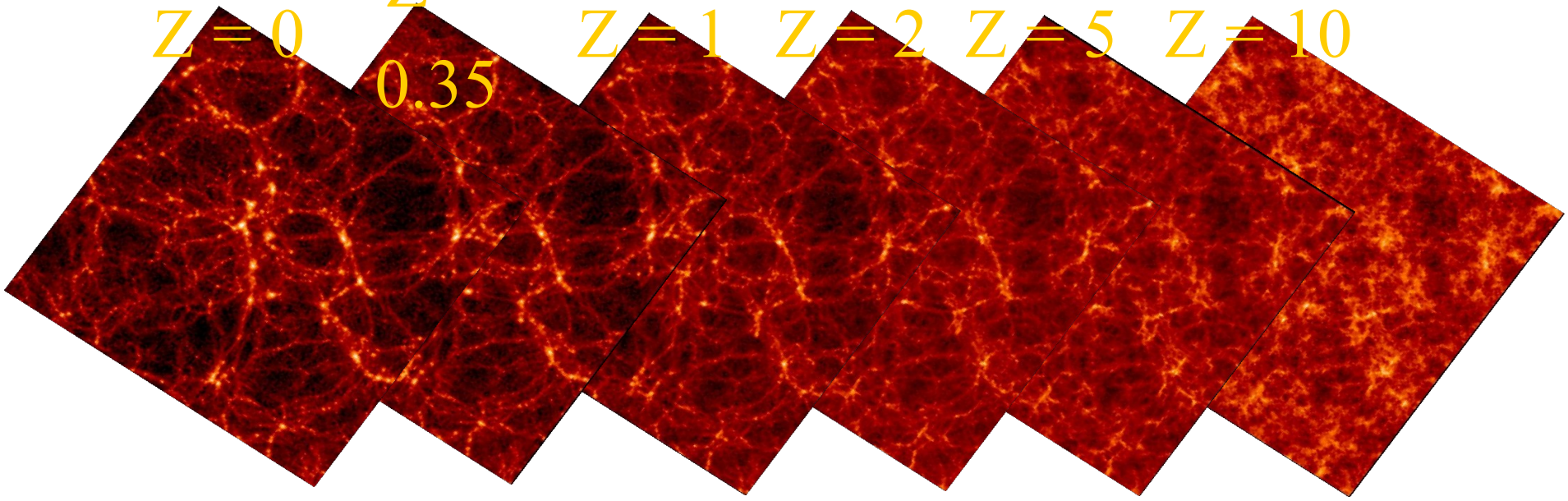

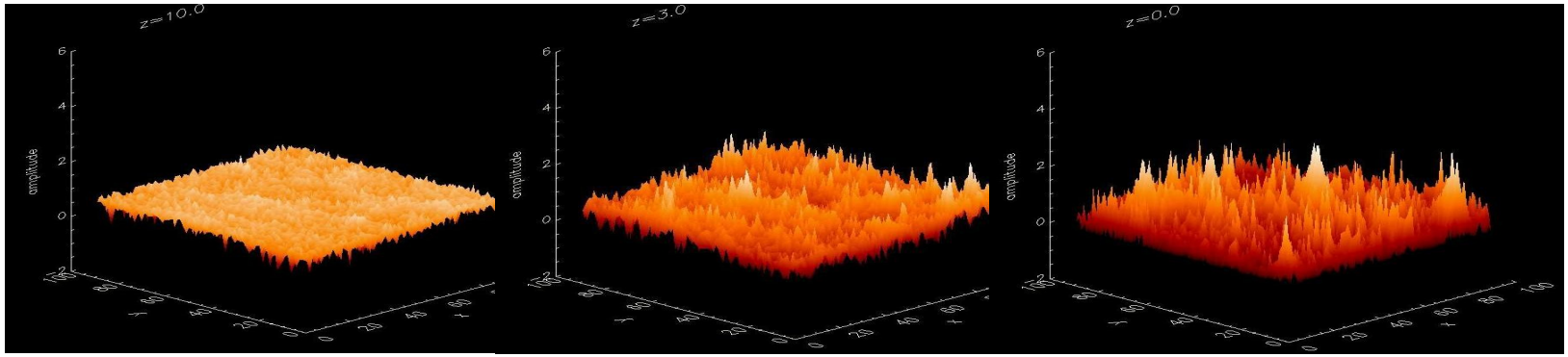

Z = 0

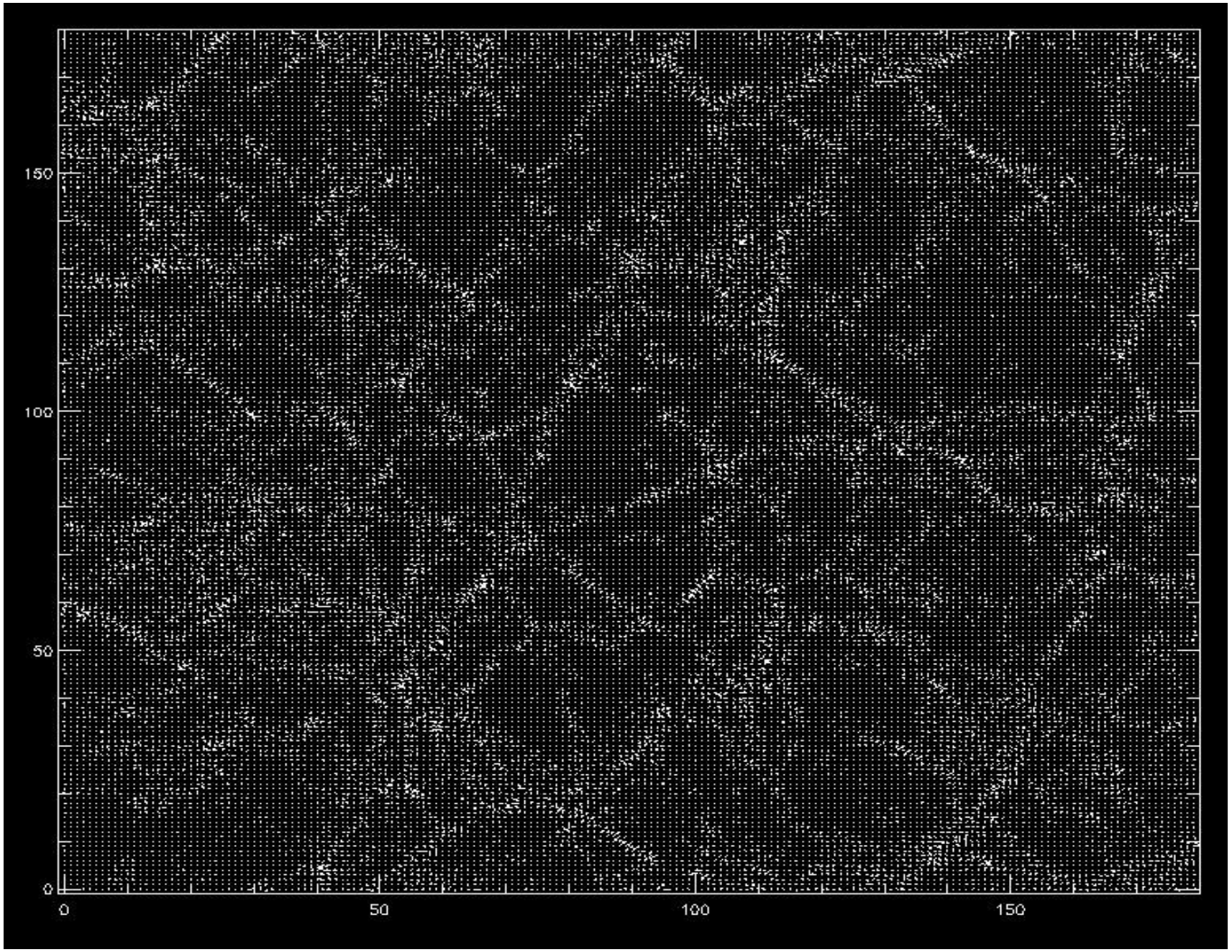

Z = 0

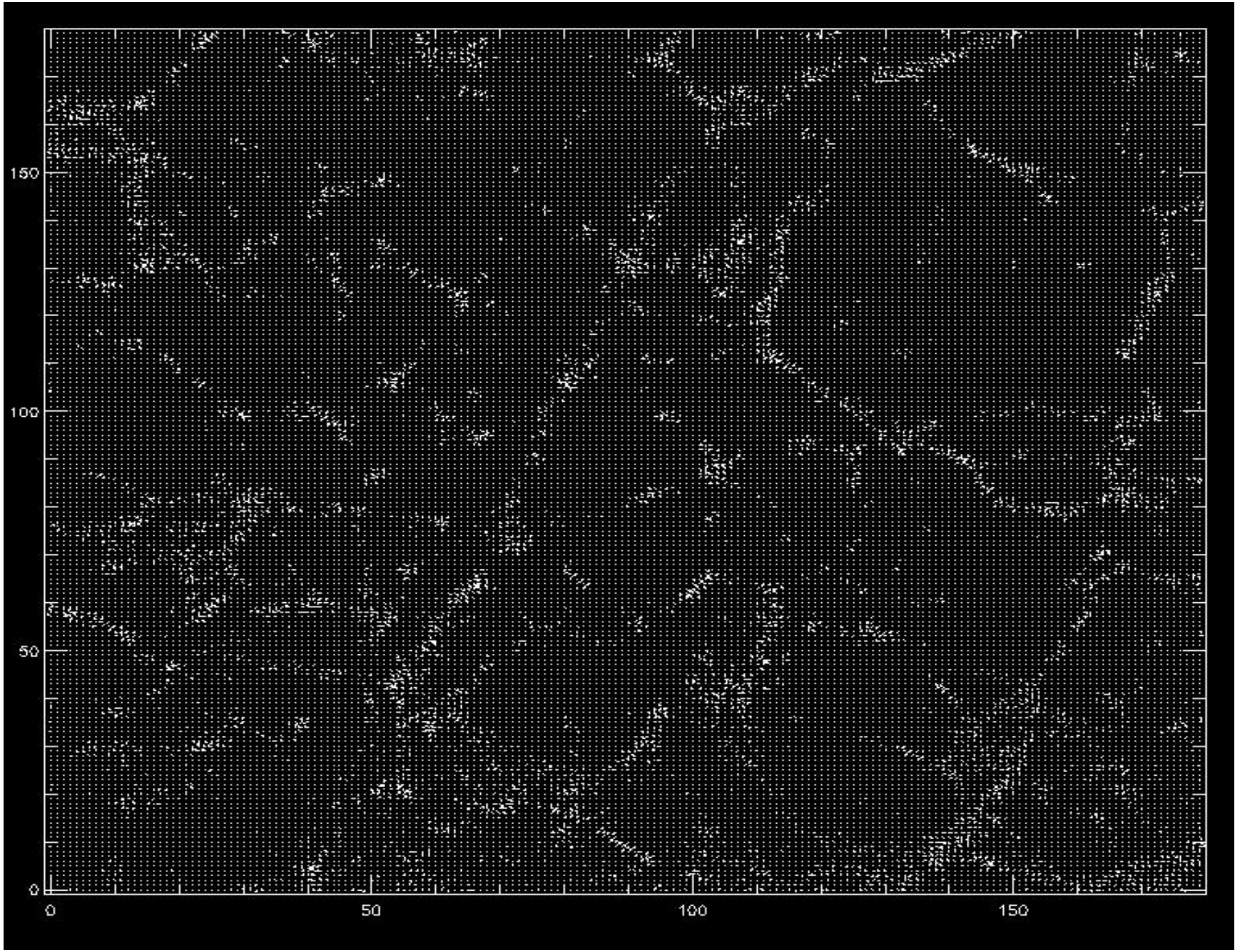

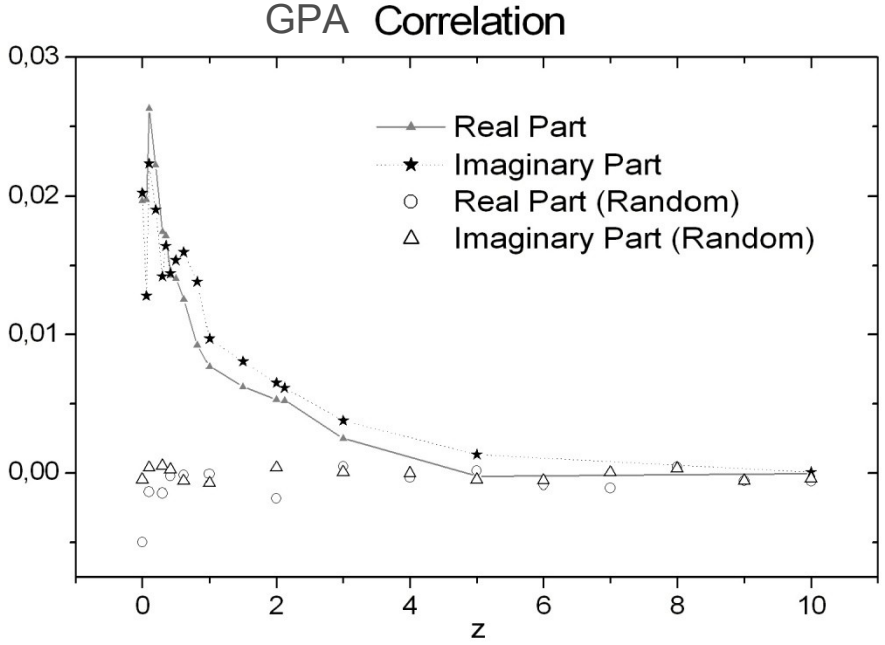
GPA Correlation
Real Part
Imaginary Part
Real Part (Random)
Imaginary Part (Random)
0,03
0,02
0,01
0,00
0
2
4
6
8
10
z

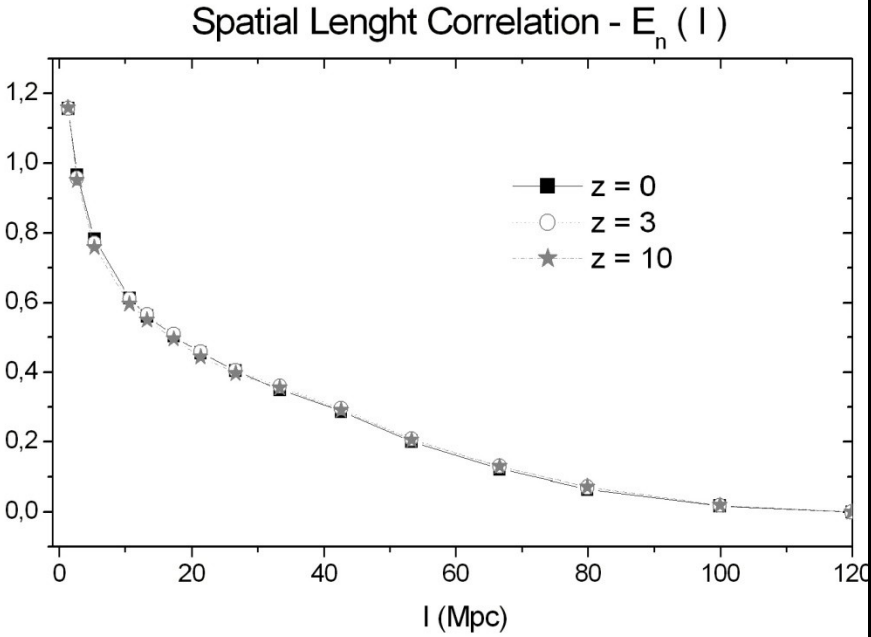
Spatial Lenght Correlation - E_n (l)
z = 0
z = 3
z = 10
1,2
1,0
0,8
0,6
0,4
0,2
0,0
0
20
40
60
80
100
120
l (Mpc)

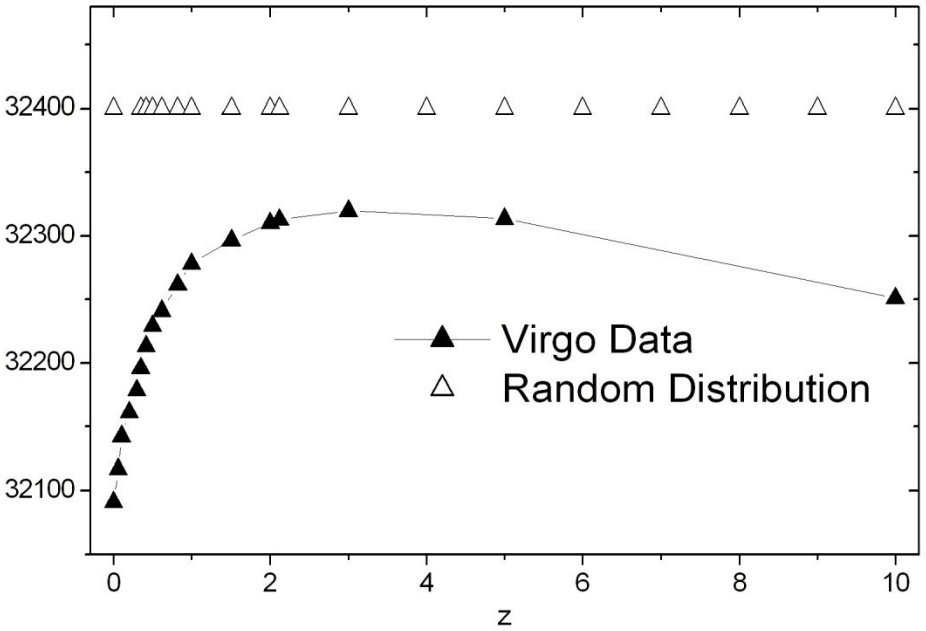
Vector Number
Virgo Data
Random Distribution
32400
32300
32200
32100
0
2
4
6
8
10
z

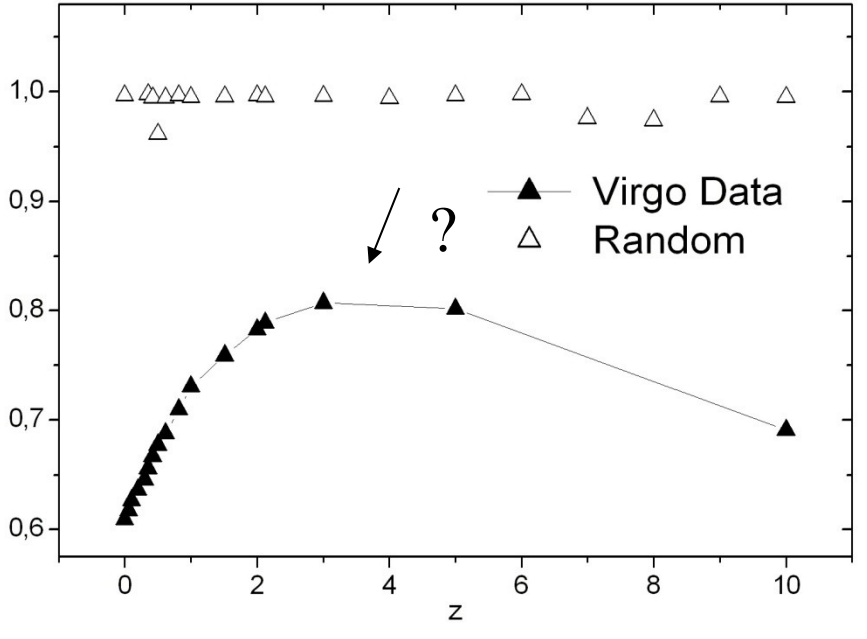
% Asymmetrical
Virgo Data
Random
?
1,0
0,9
0,8
0,7
0,6
0
2
4
6
8
10
z

$$W = nV \int \frac{Gm^2}{2r} 4\pi n r^2 \xi(r) dr \qquad (5)$$

where m is the mass of some cell, n is the average number density of particles in a cell of size V, and $\xi(r)$ is a correlation function (Wuensche et al., 2004).